Title

New carnivoran remains from the Early Pleistocene Shanshenmiaozui site in Nihewan Basin, northern China

Authors

Tong, Haowen
Zhang, Bei
Chen, Xi
et al.

Publication Date

2023-06-01

DOI

10.1016/j.quaint.2023.04.003

Peer reviewed

Quaternary International xxx (xxxx) xxx

Contents lists available at ScienceDirect

Quaternary International

journal homepage: www.elsevier.com/locate/quaint

New carnivoran remains from the Early Pleistocene Shanshenmiaozui site in Nihewan Basin, northern China

Haowen Tong [a,b,*], Bei Zhang [c], Xi Chen [d], Qigao Jiangzuo [e], Jinyi Liu [a], Xiaoming Wang [a,f]

[a] Key Laboratory of Vertebrate Evolution and Human Origins of Chinese Academy of Sciences, Institute of Vertebrate Paleontology and Paleoanthropology, Chinese Academy of Sciences, Beijing, 100044, China
[b] University of Chinese Academy of Sciences, Beijing, 100049, China
[c] National Natural History Museum of China, Beijing, 100050, China
[d] Nanjing Normal University, Nanjing, Jiangsu, 210023, China
[e] Peking University, Beijing, 100871, China
[f] Natural History Museum of Los Angeles County, Los Angeles, CA, USA

ARTICLE INFO

Keywords:
Carnivores
New fossils
Early pleistocene
Shanshenmiaozui (Nihewan, China)

ABSTRACT

In the Shanshenmiaozui (SSMZ) fauna from Nihewan Basin, *Canis chihliensis*, *Nyctereutes* sp., *Homotherium* sp., *Acinonyx* sp., *Lynx shansius* and *Pachycrocuta licenti* have been identified. *C. chihliensis* is the dominant and best represented species whose fossil materials include crania, mandibles and postcranials, including nearly complete manus and pes. The giant cheetah *Acinonyx* sp. is only represented by postcranial skeletons (scapula, radius, proximal ulna and an almost complete manus), which represent the richest collection for its kind ever known in China. *Nyctereutes* sp. is only represented by a partial cranium and distal part of a humerus. *Homotherium* sp. is only represented by a partial lower m1. *Lynx shansius* is represented by a nearly complete mandible with p3 and m1 preserved in situ. The fossil materials of *Pachycrocuta licenti* include a juvenile mandible with dp2–4 and m1 attached, an isolated dp4 and a partial ascending ramus. The SSMZ carnivoran guild resembles those of the classic Nihewan fauna (CNF) and the Dmanisi fauna, which means they probably have a similar geologic age or slightly younger of the SSMZ fauna; and they also share the same open grassland/shrubland habitat. The postcranial bones of *C. chihliensis* and *Acinonyx* sp. from SSMZ represent the first records for their kinds in China.

1. Introduction

Nihewan (=Nihowan) Basin is situated in Yangyuan County of Hebei Province in northern China (Fig. 1), which is famous for its Late Cenozoic fluvio-lacustrine deposits and the Early Pleistocene mammalian assemblage known as the Nihewan fauna (or Xiashagou fauna). The Nihewan fauna was discovered and excavated in the 1920s by Emile Licent, and was first published by Teilhard de Chardin and Piveteau (1930). The early excavations were conducted mainly in the areas around the Xiashagou (XSG) and Nihewan (NIH) villages on the north bank of the Sangganhe River (Sangkanho).

In the past decade, extensive explorations and excavations have resulted in the recoveries of new localities and much more mammalian fossils. Almost all of the recently discovered localities are located at the southern bank of the Sangganhe River, among them the Shanshenmiaozui (SSMZ) site is one of the most productive sites in mammalian fossils. Up to now, around 24 species, including undeterminable species, have been recognized and/or published: *Allactaga sibirica*, *Ochotonoides complicidens*, *Ochotona youngi*, *Canis chihliensis*, *Nyctereutes* sp., *Homotherium* sp., *Acinonyx* sp., *Lynx* sp., *Pachycrocuta licenti*, *Mammuthus trogontherii*, *Hipparion* sp., *Equus sanmeniensis*, *Coelodonta nihowanensis*, *Elasmotherium peii*, *Sus lydekkeri*, *Paracamelus gigas*, *Nipponicervus elegans*, *Eucladoceros boulei*, *Elaphurus bifurcatus*, *Spirocerus wongi*, *Gazella sinensis*, *Ovis shantungensis*, *Megalovis piveteaui*, *Bison palaeosinensis* (Tong et al., 2021), whose carnivorans are further updated in this paper. The SSMZ fauna is dominated by the following species: *Canis chihliensis*, *Mammuthus trogontherii*, *Equus sanmeniensis*, *Coelodonta nihowanensis*, *Sus lydekkeri*, *Eucladoceros boulei*, *Spirocerus wongi*, *Gazella sinensis* and *Bison palaeosinensis*, most of which have been published (Tong, 2012; Tong and Wang, 2014; Tong et al., 2011a, 2012, 2014,

* Corresponding author. Key Laboratory of Vertebrate Evolution and Human Origins of Chinese Academy of Sciences, Institute of Vertebrate Paleontology and Paleoanthropology, Chinese Academy of Sciences, Beijing, 100044, China.
E-mail address: tonghaowen@ivpp.ac.cn (H. Tong).

https://doi.org/10.1016/j.quaint.2023.04.003
Received 27 January 2023; Received in revised form 30 March 2023; Accepted 10 April 2023

2017, 2018, 2020, 2021; Tong and Chen, 2016; Chen and Tong, 2017; Tong and Zhang, 2019). Although the carnivore guild in the SSMZ fauna is not very diverse or well represented, except *C. chihliensis*, we still recognized the following taxa: *Nyctereutes* sp., *Homotherium* sp., *Acinonyx* sp. and *Lynx shansius* in addition to *C. chihliensis*; the latter has been published by Tong et al. (2012, 2020), the other taxa and new specimens of *C. chihliensis* are described in the present paper.

The SSMZ site lies at the opposing slope of Xiaochangliang (XCL), the most iconic Paleolithic Site currently in Nihewan Basin. Our stratigraphic correlation shows that the fossil-bearing sand-silt bed at SSMZ site is a little higher than the cultural layer at XCL site (Tong et al., 2011a; Liu et al., 2016), whose paleomagnetic age is about 1.36 Ma BP (Zhu et al., 2001). But the SSMZ fauna is very similar to the classic Nihewan fauna in faunal composition, which means the SSMZ fauna should have a similar age as the latter (Tong et al., 2021) or somewhat younger, whose up-dated paleomagnetic age is 2.2–1.7 Ma (Liu et al., 2012) or ~2.4–1.8 Ma (Farjand et al., 2023).

2. New fossil materials

The details of all of the studied specimens from SSMZ are listed in Table 1, which are reposited in the IVPP collection.

3. Methods, terminology and abbreviations

The suprageneric classification is mainly after McKenna and Bell (1997); The classification and anatomic terms of the Canidae are according to Evans and Christensen (1979), Wang et al. (2004), Tedford et al. (2009), and Brugal and Boudadi-Maligne (2011). The classification and dental terms as well as character analysis for Hyaenidae is after Werdelin and Solounias (1991).

The method of osteometry and osteological terms for felid are after Merriam and Stock (1932), Werdelin and Solounias (1991), Salesa et al. (2010) and Morales and Giannini (2013). The specimens were measured according to the methods used by von den Driesch (1976). The linear measurements were taken with slide calipers in millimeters. The CT scan of the mandible of *Pachycrocuta* was conducted using the high-resolution X-ray computed tomography (GE phoenix v|tome|x m380&180).

Capital letters are used for upper teeth and lowercase letters for lower teeth respectively. The biochronological framework follows Tong et al. (1995) and Qiu (2006).

Institutional and locality abbreviations: CAS, Chinese Academy of Sciences; **CNF**, classic Nihewan fauna; **DG**, Dege; **DMN**, Dmanisi; **GWL**, Gongwangling; **HX**, Hexian; **IVPP**, Institute of Vertebrate Paleontology and Paleoanthropology, CAS; **JNS**, Jinniushan; **JS**, Jianshi; **LD**, Longdan; **LGC**, Liucheng *Gigantopithecus* Cave; **Loc**, Locality; **OV**, Prefix to the Catalogue numbers of extant specimens in IVPP; **NHW**, Nihewan; **SG**, Shigou; **SSMZ**, Shanshenmiaozui; **SV**, Saint-Vallier; **TZD**,

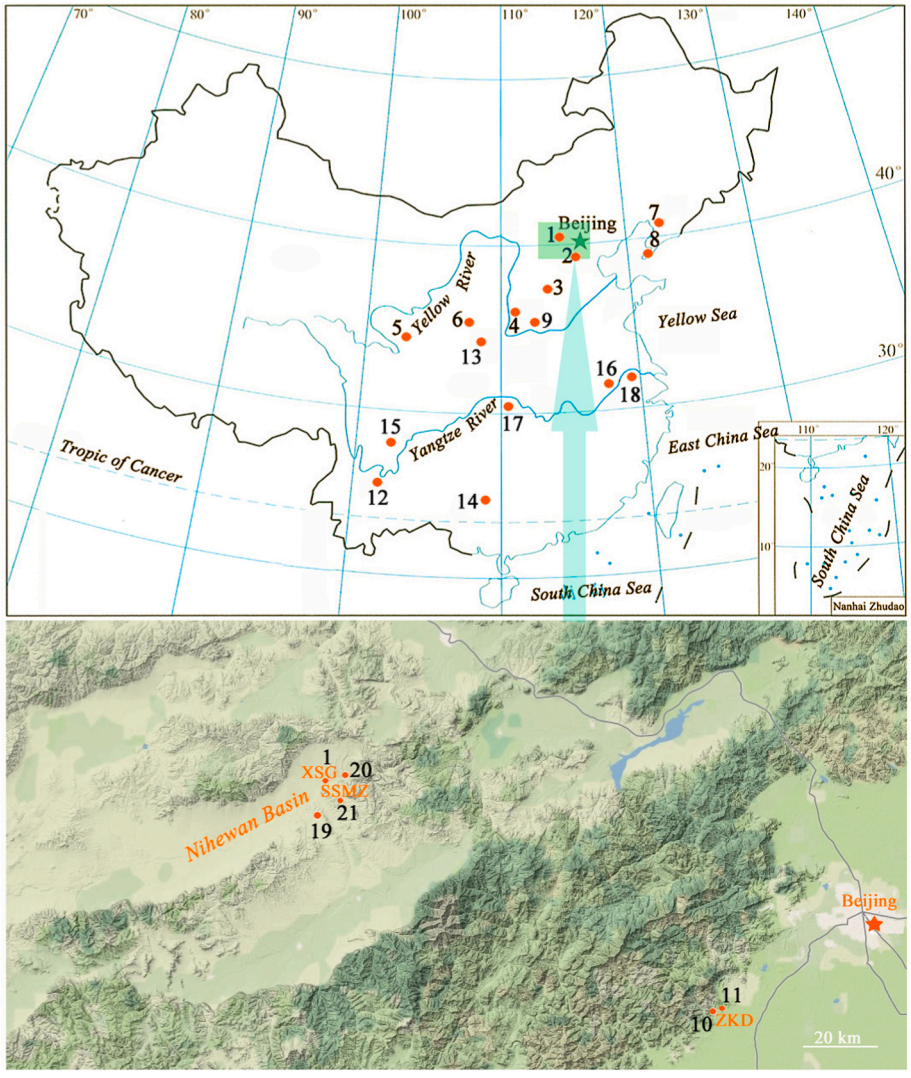

Fig. 1. Location of Shanshenmiaozui (SSMZ) site and related fossil sites in China
1 – Xiashagou of Nihewan; 2 – Zhoukoudian-Loc.1; 3 – Yushe; 4 – Xihoudu; 5 – Longdan; 6 – Bajiazui; 7 – Jinniushan; 8 – Jinyuandong; 9 – Yuanqu; 10 – ZKD-Loc.13; 11 – ZKD-Upper Cave; 12 – Yuanmou; 13 – Gongwangling; 14 – Liucheng *Gigantopithecus* Cave; 15 – Dege; 16 – Hexian; 17 – Jianshi; 18 – Tuozidong; 19 – Yangshuizhan of Nihewan; 20 – Shigou of Nihewan; 21 – Shanshenmiaozui. All of the sites (except 4, 6 and 8) yield cheetah fossils.

Table 1
Studied specimens of carnivorans from SSMZ, with context information.

Materials	Field No.	Catalog No. of IVPP	Context information
Canis chihliensis			
Incomplete skull with left I2-M2, right P1-3	N-17-092	V 31910	I15-15
Mandible with i1-m3	Surface collected[a]	V 31911	?
Atlas	N-11-184	V 31912	H23-9
Left humerus (proximal part missing)	N-16-123	V 31913.1	L19-16
Left radius	N-11-240-9a	V 31913.2	E20-8
Left ulna	N-11-240-9b	V 31913.3	E20-8
Left manus	N-11-240-10	V 31914. (1–18)	E20-8
***Nyctereutes* sp.**			
Fragment of cranium	N-15-148	V 31915	H28-5
Distal part of left humerus	N-16-107	V 31916	K19-13
Lynx shansius			
Left mandible with damaged p3 and m1	N-18-127	V 31917	J10-14
***Acinonyx* sp.**			
Right scapula	N-17-141	V 31918.1	L17-17
Left radius	N-17-132	V 31918.2	K17-17
Left ulna (lacking distal part)	N-17-117	V 31918.3	K17-15
Phalanx I of digit IV of manus	N-17-108	V 31918.4	K17-15
Left scapholunar	N-17-139-01	V 31918.5	L17-17
Left cuneiform	N-17-139-02	V 31918.6	L17-17
Left pisiform	N-17-139-03	V 31918.7	L17-17
Left trapezium	N-17-139-04	V 31918.8	L17-17
Left trapezoid	N-17-139-05	V 31918.9	L17-17
Left magnum	N-17-139-06	V 31918.10	L17-17
Left unciform	N-17-139-07	V 31918.11	L17-17
Left prepollex	N-17-139-08	V 31918.12	L17-17
Left Mc I	N-17-139-09	V 31918.13	L17-17
Left Metacarpal II	N-17-139-10	V 31918.14	L17-17
Left Metacarpal III	N-17-139-11	V 31918.15	L17-17
Left Metacarpal IV	N-17-139-12	V 31918.16	L17-17
Left Metacarpal V	N-17-139-13	V 31918.17	L17-17
Left Phalanx I of digit I of manus	N-17-139-14	V 31918.18	L17-17
Left Phalanx I of digit II of manus	N-17-139-15	V 31918.19	L17-17
Left Phalanx I of digit III of manus	N-17-139-16	V 31918.20	L17-17
Left Phalanx I of digit IV of manus	N-17-139-17	V 31918.21	L17-17
Left Phalanx I of digit V of manus	N-17-139-18	V 31918.22	L17-17
Left Phalanx II of digit II of manus	N-17-127	V 31918.23	K17-17
Left Phalanx II of digit III of manus	N-17-139-19	V 31918.24	L17-17
Left Phalanx II of digit V of manus	N-17-105	V 31918.25	K17-15
Left ungual phalanx of digit I of manus	N-17-139-20	V 31918.26	L17-17
Left ungual phalanx of digit II of manus	N-17-151	V 31918.27	L17-17
Left ungual phalanx of digit V of manus	N-17-124	V 31918.28	K18-15
Left sesamoid	N-17-139-21	V 31918.29	L17-17
Left sesamoid	N-17-139-22	V 31918.30	L17-17
Left sesamoid	N-17-139-23	V 31918.31	L17-17
Left sesamoid	N-17-139-24	V 31918.32	L17-17
Left sesamoid	N-17-139-25	V 31918.33	L17-17
Left sesamoid	N-17-139-26	V 31918.34	L17-17
Left sesamoid	N-17-139-27	V 31918.35	L17-17
Left sesamoid	N-17-139-28	V 31918.36	L17-17
Right Mt. V	N-17-128	V 31918.37	K17-17
?Phalanx I of digit V of pes	N-17-106	V 31918.38	K17-15
?Phalanx I of digit IV of pes	N-17-137	V 31918.39	K17-17
***Homotherium* sp.**			
Partial left m1	N-17-039	V 31919	K18-12
Pachycrocuta licenti			
Partial right mandible with dp2-4 and m1	N-06-090	V 31920	D5-7
Isolated right dp4	N-18-167	V 31921	K13-16
Partial mandible with broken ramus and condyle as well as angular process	N-08-064	V 31922	H16-4

[a] Collected by Wei Qi.

Tuozidong; **UC**, ZKD-Upper Cave; **UMF**, Untermassfeld; **V**, Prefix in the catalog numbers for vertebrate fossils in IVPP; **XSG**, Xiashagou; **YM**, Yuanmou; **YQ**, Yuanqu; **ZKD**, Zhoukoudian (=Choukoutien).

Morphological abbreviations: APD: anteroposterior diameter; **Cu:** cuneiform; **L:** length; **Mc**: metacarpal; **Mg:** magnum; **Mt:** metatarsal; **Pis:** pisiform; **Pp:** prepollex; **Scl:** scapholunar; **Td:** trapezoid; **TD:** transverse diameter; **Tz:** trapezium; **Un:** unciform; **W:** width.

4. Systematic paleontology

Class Mammalia Linnaeus, 1758
Order Carnivora Bowdich, 1821
Suborder Caniformia Kretzoi, 1943
Family Canidae Batsch, 1788
Subfamily Caninae Batsch, 1788
Genus *Canis* Linnaeus, 1758

***Canis chihliensis* Zdansky, 1924.**
(Fig. 2).

Diagnosis (emended from Zdansky, 1924; Tong et al., 2012, 2020; Jiangzuo et al., 2018): Large body size; sagittal crest high and long; elongated rostrum; I3 robust; P4 elongated and with well-developed protocone, with its medial ridge mostly connected to anterior ridge of paracone; M1 strongly mesiodistally compressed with broad cingular hypocone, medial ridge of paracone and metacone mostly present; M2 and m2 large relative to M1 and m1 respectively; reduced metaconid on m1; lower LP/LP4M ratio; p4 as high as m1 paraconid; robust p4–m1 complex for cracking bone; pentadactyl manus and tetradactyl pes.

Materials: Incomplete skull with left I2-M2 and right P1-3 (V 31910), mandible with i1-m3 (V 31911), atlas (V 31912), left humerus (proximal part missed) (V 31913.1); left radius (V 31913.2), left ulna (V 31913.3), left manus (V 31914).

Descriptions.

Skull and mandible: All the dental characters and measurements of the here described specimens are exactly the same as those by Tong et al. (2012); but both the upper (Fig. 2: 1A) and lower (Fig. 2: 3C) dentitions of the new materials are much better preserved and represent the most

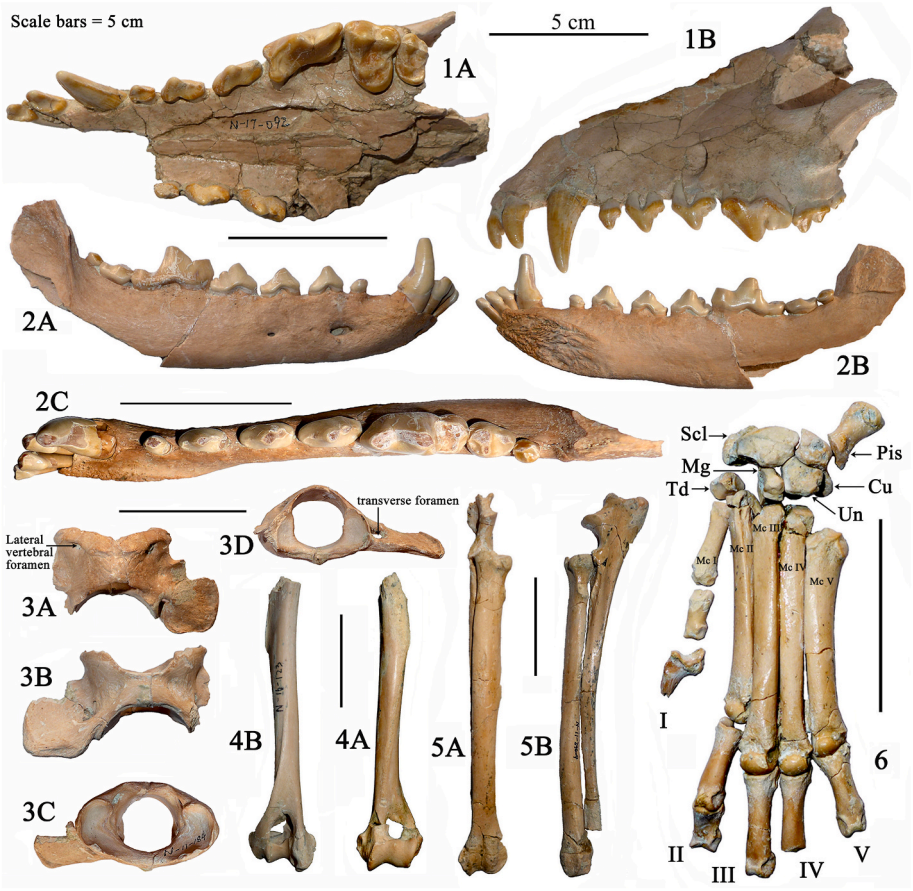

Fig. 2. *Canis chihliensis* from SSMZ
1A-1B – incomplete skull with left I2-M2 and right P1-3 (V 31910); 2A-2C – right mandible with i1-m3 (V 31911); 3A-3D – partial atlas (V 31912); 4A-4B – left distal humerus (V 31913.1); 5A-5B – left radius (V 31913.2) and ulna (V 31913.3); 6 – left manus (V 31914).

complete dentitions for this species.

I2 has both medial and lateral cusplets; I3 is caniniform and much bigger than I2, and lacks the cusplets, but with a prominent slanting lingual cingulum; P1 is single-rooted, P2 and P3 are double-rooted. The I3–C diastema and C–P1 diastema are equally spaced; the diastemas between adjacent premolars are prominent. For the P3 and p4, each has two posterior cusplets; P4 has a small but distinct protocone; M1 has a well-developed parastyle but less developed anterior cingulum; entoconid on m2 is completely absent.

Dimensions: Upper dental length (I2-M2) is 117.0; upper premolar series length is 61.1; upper molar series length is 23.8; L × W of P4 is 22.9 × 12.2; L × W of M1 is 14.4 × 18.8; L × W of M2 is 9.6 × 13.2; M1-M2 length is 23.1. Mandibular toothrow length (i1-m3) is ~116.4; lower premolar series length is 48.7; lower molar series length is 40.1; L × W of m1 is 24.4 × 9.6. The index (LP4 × 100/LM1+M 2) is 99.

Atlas: The left wing of the transverse process is broken off, while the right one is almost complete. The neural arch (or dorsal arch) and the body of atlas are well preserved. In dorsal view (Fig. 2: 3A), a crest or a rim along the frontal edge of the neural arch can be seen, which is slightly concave anteriorly; there is an atlantal foramen (or lateral vertebral foramen or alar foramen) at each side behind the front crest; in the posterior part, there is a transverse foramen at each side; the dorsal tubercle is not so prominent; the posterior outline is markedly concave posteriorly. In ventral view, both the anterior and posterior articular facets are strongly concave; the transverse foramen is located at the root part of the transverse process; the ventral tubercle is undeveloped. In cranial view, the neural canal is big and has a larger height than width; there is a kidney-shaped articular facet for the occipital condyle at each side of the neural canal, and the articular surfaces are spoon-like. In caudal view, there is also a kidney-shaped articular facet for axis at each side of the neural canal, but slightly smaller and less concave relative to the cranial ones; the posterior opening of the transverse foramen can be seen.

Dimensions: The least dorsal length along the midline is 14.3 and the maximum length is 40.6; the width is 40.8 × 2 = 81.6; the height is 27.3; the widths of the anterior and posterior articular facets are 41.8 and 32.7 respectively; the least ventral length along the midline is 10.9.

Humerus: Although the proximal half of the bone is actually missing, the specimen (Fig. 2: 4A-4B) is more complete and better preserved than the specimen described by Tong et al. (2012). The deltoid tuberosity is quite prominent; the lower portion of the shaft is nearly straight; the distal end is fairly expanded transverely relative to the shaft; the lateral epicondylar crest is sharp; because of the breakage of the upper rim of the supratrochlear foramen, the details of the radial fossa became unclear; while the olecranon fossa seems quite deep.

Dimensions: The distal TD is 32.0; the distal APD is 26.4.

Radius: The specimen (Fig. 2: 5A-5B) is nearly complete. The proximal facet has a semilunar outline, and with the front edge posteriorly concave. The distal dorsal tubercle and the grooves for tendons of extensor digitorum and extensor carpi radialis beside it are very pronounced.

Dimensions: the total length is 160.1; the proximal and distal widths are 18.1 and 24.9 respectively.

Ulna: The specimen is nearly complete except the distal part (Fig. 2: 5A-5B). The olecranon tuber expands terminally and forked at the supra-anterior part; the olecranon tuber is robust, while the shaft is quite slim. The anconeal process and the medial coronoid process are very developed, but the lateral coronoid process is small. The trochlear notch (or

semilunar notch) is deep.

Dimensions: Total length >166; olecranon length is 29.1; smallest depth of olecranon is 6.7; greatest breadth of the proximal articular surface is larger than 14.1.

Manus: The preserved elements include scapholunar, cuneiform, pisiform, trapezoid, magnum, unciform, Mc I–V, proximal phalanges I–V, distal phalanx of digit I, and middle phalanx of digit II (Fig. 2: 6).

The scapholunar is the largest among the carpals and with a large radial facet on the top and three bottom facets for the distal carpals; the posterior portion of the cuneiform extends downward to the same level of the lower boundary of the unciform; the cuneiform facet of the pisiform only partially preserved, but the distal part is complete and strongly expanded; the unciform has an irregular anterior face but a triangular distal face; the magnum and trapezoid are much smaller than other carpals and irregular in form. The Mc V is the second shortest metacarpal after the Mc I, but much robuster and dorsoventrally flattened than the others. In the metacarpals, their proximal articular surfaces for the distal carpals have longer anteroposterior dimensions than transverse ones; while the head or distal end is different, Mc II and IV has almost symmetric head, while the others has asymmetric head, but the palmar keels or sagittal crest of the distal articulation are equally developed at the disto-volar aspect, both high and sharp, except in Mc I. The only claw bone, a distal phalanx of digit I, has undeveloped or unpreserved ungal crest, and the ungal process is not so long but stout.

The length of metcarpals I–V are 22.6, 59.1, 68.4, 68.0 and 57.5 respectively; the length of the proximal phalanges of digital I–V are 13.4, 23.6, 27.6, >21.9 and 22.7 respectively; the length of the distal phalanx of digit I is 16.1; the length of the middle phalanx of digit II is 14.1. The manus bone is smaller than the specimens described earlier by Tong et al. (2012).

Comparisons and discussions: The new specimens can be attributed to the species *Canis chihliensis* according to their size and morphological characters. The maxillary and the mandibular toothrows as well as the manus bones of this paper represent the most complete ones for *C. chihliensis* ever uncovered. Although *Canis chihliensis* is slightly smaller than the extant local grey wolf (*Canis lupus chanco*), it is among the largest canine animals of its time in China. Compared with the three species of *Canis* from Longdan (Qiu et al., 2004), the *C. chihliensis* from SSMZ has more pronounced protocone on P4, relatively large M2 and m2, but reduced metaconid on m1 and other lingual cuspids on the lower molars.

Concerning the P4/M1+M2 length ratio, it is not a reliable index to define *C. chihliensis*, because the value is not always less than one (i.e. P4 is shorter than the M1+M2 length) as originally proposed by Pei (1934: P.13); on the contrary, it is quite often for *C. variabilis* and *C. lupus* to have this ratio less than one as noticed by the present authors.

In the XSG fauna, three types of *Canis* were originally recognized: typical *Canis chihliensis*, *Canis chihliensis* form *palmidens* and *Canis chihliensis* form *minor* (Teilhard de Chardin and Piveteau,1930); the last one was transferred to *Eucyon* but retaining the species name (Tedford and Qiu, 1991), while the second one was promoted to species status by Tedford et al. (2009). The most recent study shows that "it is very difficult to distinguish *C. chihliensis* from *C. palmidens* with clear cut"; "therefore, the two forms are viewed as single population (*Canis chihliensis*)" (Jiangzuo et al., 2018). Compared with the XSG specimens of *C. chihliensis* from the classical Nihewan fauna, the dental size of the new materials is slightly larger but with significant overlap. Among the morphological traits, one notable difference is the more reduced lingual cuspids on m1. According to the morphotype defined by Jiangzuo et al. (2018), 5 types are distinguished, and type 1 represents the entoconid as large as the hypoconid, and type 5 represents entoconid totally reduced to cingulid-like, with 2–4 successively intermediate. The morphotype ranges from 3 to 5 in the SSMZ population, with type 4 dominant (n = 10), whereas in the Xiashagou population, the morphotype ranges from 1 to 4, with 2, and 3 dominant (n = 27). These imply a more reduced entoconid in the SSMZ population, and probably suggest a slightly younger age of the SSMZ fauna than the XSG assemblage.

During the Early Pleistocene in China, the tribe Canini underwent an evolutionary explosion, with the highest diversity in its history. Concerning the genus *Canis*, more than 6 species of Early Pleistocene age have been identified, namely *Canis antonii* and *C. chihliensis* (Zdansky, 1924), *C. teilhardi*, *C. longdanensis* and *C. brevicephalus* (Qiu et al., 2004), and *C. palmidens* (Teilhard de Chardin and Piveteau, 1930) (Tedford et al., 2009), most of them have smaller body mass than the extant *C. lupus* but much bigger than *Cuon* (Bartolini-Lucenti and Spassov, 2022). A critical review of these species, however, is required to examine the validity of such a high diversity. The three recently established species from the Longdan fauna share some similar characters, i.e., the main cusps on the upper M1 are tubercle-like, the protocone on P4 is reduced, and the M2 and m2 are small relative to M1 and m1 respectively; but the teeth of *C. brevicephalus* are prominently larger.

During the Early Pleistocene in Europe, the situation is quite similar to that of China, i.e. a couple of *Canis* species abruptly appeared at ca. 2 Ma (Bartolini-Lucenti et al., 2017), which is regarded as the "wolf event" and used as the marker of the beginning of the Quaternary Period in Western Europe (Azzaroli, 1983; Sardella and Palombo, 2007). The "wolf event" means the radiation of canids referable to *Canis* ex gr. *C. etruscus*. Cherin et al. (2014a) re-defined the species C. *etruscus* and gave an extensive revision of the diagnostic characters of the species, which regarded the species *C. chihliensis* of Nihewan as one synonym of the species *C. etruscus*. But our study shows that *C. chihliensis* is different from *C. etruscus* in its larger and less transversely compressed cheek teeth (Tong et al., 2012). *Canis etruscus* appeared in Europe at about 2 Ma (Cherin et al., 2013) and was limited only to Early Pleistocene (Brugal and Boudadi-Maligne, 2011). Furthermore, the P4 dimensions of the Early Pleistocene *Canis* species in Europe are markedly smaller than those of the extant grey wolf *C. lupus* (Brugal and Boudadi-Maligne, 2011). Concerning the phyletic relationships between *C. mosbachensis* and *C. lupus*, these two taxa are expressed by a mosaic of characters not yet firmly defined (Mecozzi et al., 2017).

The Chinese Middle Pleistocene *Canis* are mainly (or exclusively by Jiangzuo et al., 2018) referred to the species *C. variabilis* or *C. mosbachensis variabilis* by Jiangzuo et al. (2018). Although *C. variabilis* has a very wide variation in body size, it's generally smaller than *C. lupus* (Teilhard de Chardin and Pei, 1941; Tong et al., 2012). Although it is true that the corresponding dimensions of *C. chihliensis* from SSMZ (Tong et al., 2012) fall within the range of *C. variabilis* (Pei, 1934; Teilhard de Chardin and Pei, 1941), but they are generally larger than those of the latter (Tong et al., 2012). Moreover, *C. chihliensis* is similar to *C. variabilis* both in size and form, and both of them are distinctly smaller than *C. lupus* (Tong et al., 2012; Jiangzuo et al., 2018). Therefore, it must be careful to distinguish the Middle Pleistocene *Canis* species from those of the Early Pleistocene based on size only. The Chinese Late Pleistocene *Canis* only had one species, *C. lupus* (Qiu, 2006).

It was regarded that *C. chihliensis* is not a well-defined species (Teilhard de Chardin and Pei, 1941) due to its great variabilities (Jiangzuo et al., 2018), it seems that the Early Pleistocene *C. chihliensis* from Nihewan are distinct enough to be an independent species, mainly because of its robust protocone on P4, prominent parastyle on M1, relatively larger M2 and reduced lingual cuspids on m1 (Tong et al., 2012). Furthermore, *C. chihliensis* has less elongated rostrum and lower LP/LP4M ratio (Jiangzuo et al., 2018) and other specialized characters such as increased cutting edges for meat consumption and robust p4–m1 complex for cracking bones (Tong et al., 2020).

Although the hypercarnivorous dentition of *C. chihliensis* shows high similarity with those of the *Lycaon*-like dogs, including all the Old World forms under the specific group *Canis* (*Xenocyon*) ex gr. *falconeri* (Rook, 1994; Martínez-Navarro and Rook, 2003) or *Canis* (*Xenocyon*) group (Bartolini-Lucenti and Spassov, 2022), while the pentadactyl manus (Fig. 2: 6) of the former makes it difficult to group them together. *Canis (Xenocyon)* ex gr. *falconeri* already developed a tetradactyl forelimb as early as the Early Pleistocene in the Pirro Nord fauna (Martínez-Navarro

and Rook, 2003), which is a trait unique to *Lycaon* among living canids (Martínez-Navarro and Rook, 2003; Hartstone-Rose et al., 2010). It is worth mentioning that the designation of *Canis* (*Xenocyon*) was a useful way to acknowledge the peculiarity of those Plio-Pleistocene taxa with extreme hypercarnivorous characteristics in the genus *Canis*, and the group was re-defined to include the following taxa: *C.* (*Xenocyon*) *africanus*, *C.* (*Xenocyon*) *antonii*, *C.* (*Xenocyon*) *brevicephalus*, *C.* (*Xenocyon*) *dubius*, *C.* (*Xenocyon*) cf. *dubius*, *C.* (*Xenocyon*) *falconeri*, *C.* (*Xenocyon*) *lycaonoides*, and *C.* (*Xenocyon*) *texanus* (Bartolini-Lucenti and Spassov, 2022). In addition, the recently established species *Canis orcensis* also is a hypercarnivorous type (Martínez-Navarro et al., 2021). This rather derived hypercarnivorous species mentioned above had an East Asian origin (Bartolini-;Lucenti et al., 2021). While in China, the hypercarnivorous canines of Pliocene-Early Pleistocene are usually grouped under the genus *Sinicuon* (Qiu et al., 2004; Wang et al., 2014; Jiangzuo, 2021; Jiangzuo et al., 2022b); and Jiangzuo et al. (2022b) even proposed two lineages for the hypercarnivorous canine taxa: *Sinicuon-Cuon* lineage and *Xenocyon-Lycaon* lineage, which means *Cuon* was derived from *Sinicuon* and *Lycaon* was evolved from *Xenocyon* respectively. Although *Cuon* resembles *Lycaon* in the reduction of lingual cusps and/or cuspids on P4 and the molars, it is different from the latter in its pentadactyl manus and loss of the lower m3. Furthermore, the latter has its metaconid on m1 less reduced. Therefore, they should have different origins. The early *Cuon*-like canids are different from the extant forms in their larger size and the presence of m3. In China, the earliest record of the living species *Cuon alpinus* is from the earliest Middle Pleistocene site ZKD Loc.13 (Teilhard de Chardin and Pei, 1941), and the living species *Cuon javanicus* from the Middle Pleistocene Yanjinggou fauna is larger and more robust than the extant form of today (Colbert and Hooijer, 1953).

Moreover, *C. chihliensis* is grouped with the *Canis* species (Tedford et al., 2009) rather than with the *Xenocyon- Sinicuon-Lycaon-Cuon* complex, and its dentition and postcranial bones support such a solution. Concerning the reduction of the lingual cuspids on the lower molars, it is just a common character shared by most of the Early Pleistocene large-sized canids, such as *Canis teilhardi* (Qiu et al., 2004).

In the SSMZ fauna, *C. chihliensis* is the most common carnivoran taxon. In particular, our SSMZ materials demonstrate the primitive presence of a first metacarpal and associated phalanges, which is different from the *Xenocyon-Lycaon* lineage whose first digit is absent (Rook, 1994: 76; Martínez-Navarro and Rook, 2003) but has a vestigial metacarpal I (Smith et al., 2020). While it is not surprising that *C. chihliensis* retains plesiomorphic in its lack of highly cursorial adaptations, the SSMZ materials nonetheless provide an important benchmark for understanding of the early evolution of *Canis* in Eurasia. It is equally interesting to note that Chinese *C. chihliensis*, especially in samples from later sites (Jiangzuo, 2021), began to show initial stages of dental hypercarnivory (Tong et al., 2012), a feature commonly

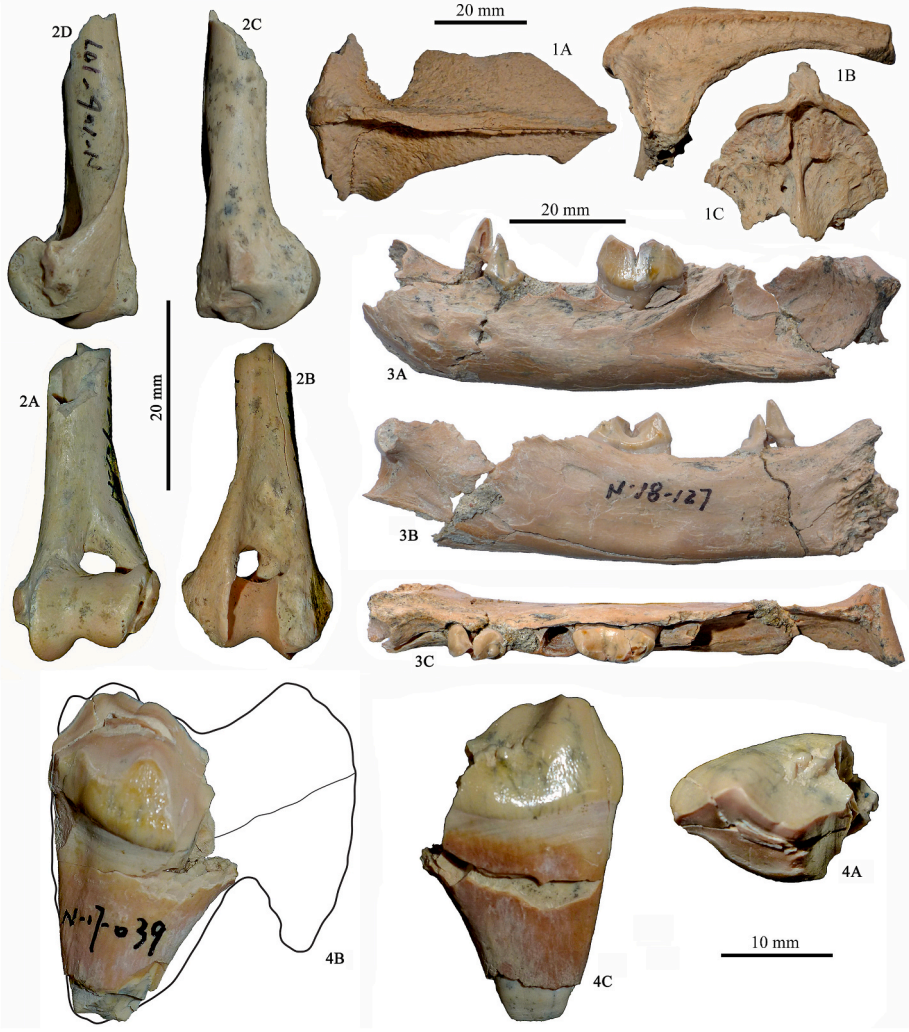

Fig. 3. *Nyctereutes* (1A-1C, 2A-2D), *Lynx shansius* (3A-3C) and *Homotherium* sp. (4A-4C) from SSMZ
1A-1C – fragment of cranium (V 31915); 2A-2D – distal part of left humerus (V 31916); 3A-3C – left mandible with damaged p3 and m1 (V 31917); 4A-4C – partial left m1 (V 31919).

associated with highly social behavior and large body size (Van Valkenburgh et al., 2004).

Genus *Nyctereutes* Temminck, 1838

***Nyctereutes* sp.**

(Fig. 3: 1A-1C, 2A-2D).

Materials: Fragment of cranium (V 31915); distal part of left humerus (V 31916).

Description.

Cranium (V 31915): The partial parietal and the supraoccipital bones are preserved. The sagittal crest is narrow and high, and its dorsal outline in lateral view is quite straight (Fig. 3:1B). The parietal surface is quite rugose, which is a typical character for *Nyctereutes* skull. The nuchal crest is rim-like (Fig. 3:1C). The external occipital protuberance is undeveloped. The external occipital crest is less developed. The surface of the supraoccipital is also rugose and concave (Fig. 3:1C). There is a groove above the external occipital crest, and there is a tiny nutrient foramen at the left side of the external occipital crest (Fig. 3:1C). The transverse canal which contains the venous transverse sinus in the supraoccipital is quite big (Fig. 3:1B).

Humerus: A partial left humerus (Fig. 3: 2A-2D) preserve the lower portion of the mid-shaft and the distal extremity, whose capitulum, trochlea, lateral and medial epicondyles can be observed. The shaft is nearly straight and flairs slightly near the medial and lateral epicondyles, and the edge flared out above the lateral epicondyles forms a thin and sharp crest (lateral supracondylar crest) (Fig. 3: 2D). In front view, the articular facet consists of the trochlea at the medial part and the capitulum at the lateral side; the medial edge of the trochlea is vertical, while the lateral edge of the capitulum is slanting medioventrally. The supratrochlear foramen (or ulnar fossa foramen) is wider than high (Fig. 3: 2A).

Dimensions: The distal TD is 16.1; the distal APD is 12.1; the mid-shaft TD is 6.7; the mid-shaft APD is 7.7.

Comparisons and discussions: Based on the rugose cranial bone surface (Teilhard de Chardin and Pei, 1941) and the smaller size of the humerus, the aforedescribed fossils can be referred to *Nyctereutes*. The humerus of the SSMZ *Nyctereutes* is markedly smaller than those of *Canis* and *Vulpes*, and even smaller than that of the extant species *N. procyonoides* (OV2111). Therefore, currently the SSMZ *Nyctereutes* fossils only can be treated as an undeterminable species of quite small size.

Raccoon dog is among the most common mammals in the Nihewan fauna, and recently a very rich collection of *Nyctereutes* was reported from the Yangshuizhan site in Nihewan Basin *senso lato* (Liu, 2019). But it is unfortunate that no postcranial bones were included in that study. The fossils of *Nyctereutes* were attributed to the species *N. sinensis* in previous publications (Teilhard de Chardin and Piveteau, 1930; Tedford and Qiu, 1991) whereas Liu's (2019) unpublished dissertation study recommends using a name *N. schlosseri* by Barbour, Licent, and Teilhard de Chardin (1926) for the Nihewan fossils and discarding the name *N. sinensis* as *nomen vanum*. However, until Liu's view is formally published, it cannot be considered a nomenclatural act regarding a name that was extremely poorly founded. The temporal range of *Nyctereutes tingi* in Nihewan Basin covers Late Pliocene and Early Pleistocene (Liu, 2019; Liu et al., 2022). It is worth mentioning that some specimens of Late Pliocene age from Yegou site near Yangshuizhan were identified as *N. sinensis* (Liu et al., 2022).

Although *Nyctereutes* was replaced by *Canis* at *ca.* 1.8 Ma in Europe (Koufos, 2014; Koufos and Kostopoulos, 2016), some European Pliocene and Early Pleistocene sites did yield the humerus of *Nyctereutes* (Argant, 2004; Bartolini-Lucenti et al., 2018), but all of the European humeri are exclusively larger than the SSMZ specimen.

Suborder Feliformia Kretzoi, 1945

Family Felidae Batsch, 1788

Subfamily Felinae Batsch, 1788

Genus *Lynx* Linnaeus, 1758

***Lynx shansius* Teilhard de Chardin et Leroy, 1945**

(Fig. 3: 3A-3C; Table 2).

Materials: Left mandible with damaged p3 and m1 (V 31917) (Fig. 3: 3A-3C).

Descriptions: The mandible is seriously fragmented; the anterior teeth and p4 are missed; p3 and m1 are fragmented; the mandibular body is nearly complete. In lateral view (Fig. 3: 3A), there are two equally developed mental foramina, the anterior one is under the diastema, while the posterior one is under p3. The p3 has a high principal cuspid and a quite prominent posterior cusplet, while the anterior cusplet is tiny; while the anterior cusplet is vestigial. The m1 has both paraconid and protoconid developed, but the metaconid is vestigial; but the apex of the protoconid is broken off. The carnassial notch is V-shaped in buccal view and stops halfway down the crown. Moreover, the new specimen from SSMZ seems distinct in its straighter inferior border of the mandibular body.

Comparisons and discussions: The Chinese lynx, both fossil and extant forms, have approximately the same size (see Table 2). The lynx fossils from Nihewan Basin were once referred to the following species: *Felis* (*Lynx*) sp. (Teilhard de Chardin and Piveteau, 1930), *Lynx shansius* (Teilhard de Chardin and Leroy, 1945) and *Lynx variabilis* (Tang, 1980). More recently, Qiu et al. (2004) included the ever reported lynx fossils of Nihewan Basin into the same species, i.e., *L. shansius*, which is characterized in its robust skull and prominent metaconid on m1 (Teilhard de Chardin and Leroy, 1945); whereas, it was often treated as a subspecies *L. issiodorensis shansius* (Werdelin, 1981). Concerning the Chinese *Lynx* species of Middle Pleistocene onward, it is still controversial; the felids of the lynx size from the Middle Pleistocene Peking Man site (ZKD Loc. 1) at Zhoukoudian were classified into two groups: the species *Felis teilhardi* and the *Felis* sp. 2 (Pei, 1934); the former is a distinct species because of its presence of a P2 and oval-shaped p4, as well as relatively smaller size than the extant lynx; while the latter is closer to *Lynx* in its deep mandibular body and elongated p4.

In sum, the SSMZ lynx fossil can be referred to the species *Lynx shansius* according to its form and size, which is larger than the newly erected species *Lynx hei* (Jiangzuo et al., 2022a,b,c). The rudimentary metaconid on m1 is similar to the XSG specimen but much weaker than those of *Lynx shansius* from Longdan.

Subfamily Acinonychinae Pocock, 1917

Genus *Acinonyx* Brookes, 1828

***Acinonyx* sp.**

(Fig. 4; Tables 3 and 4).

Materials: Right scapula (V 31918.1), left radius (V 31918.2), left ulna (distal part broken off) (V 31918.3), left manus (V 31918.4–36), right Mt. V (V 31918.37), left phalanx I (V 31918.39), left phalanx I (V 31918.38), left phalanx I (V 31918.4).

Descriptions:

Scapula: The lower part of the scapular spine, including the acromion, were broken off, other parts are well preserved. The shoulder blade has a felid-form, but slightly narrower than usual in fore and aft direction, especially in the ventral portion; the supra-caudal corner or teres process is nearly rectangular (Fig. 4: 1A). The epiphyseal lip is roundish; the thoracic angle or caudal angle is projected; the cervical angle is like a gentle slope. The thin cervical edge presents a scapular notch near the distal end, which is more concave than in the extant *A. jubatus*. The caudal border is nearly straight, while the cranial and dorsal borders are convexly curved. The crest of spine divides the shoulder blade into two equal parts approximately, i.e., the supraspinous and infraspinous fossae; and the spine is slightly carried backward over the infraspinous fossa. The feature of the acromion process is unclear. The scapular neck is narrow, and on its medial aspect, there

Table 2
Measurements of *Lynx shansius* from SSMZ, compared with related species (in: mm).

Taxa		*Lynx shansius*	*Felis* (*Lynx*) sp.	*Lynx shansius*	*Lynx shansius*	*Lynx lynx*	*Lynx lynx*
Geologic age		Early Pleistocene	Early Pleistocene	Early Pleistocene	Early Pleistocene	Late Pleistocene	Extant
Sources		V 31917(This paper)	Teilhard de Chardin and Piveteau (1930)	Teilhard de Chardin and Leroy (1945)	Qiu et al. (2004)	Pei (1940)	OV1470 (This paper)
C	L	10.0 (at alveolus)	9.0		9.4–10		9.2
	W	8.0 (at alveolus)	8.0		7.7–8.0		6.5
p3	L	10.0	9.0		9.5–10.2		9.7
	W	5.9			5.0–6.0		5.1
p4	L	11.8 (at alveolus)	13.0	11.2	11.9–12.9		11.4
	W	6.6 (at alveolus)			5.5–6.8		6.1
m1	L	14.0	14.5	14.0	14.9–15.6	15.1–16.2	14.9
	W	6.6			6.4–7.0	7.2–7.3	6.9
Length of diastema (c-p3)		9.9			11–11.7		12.1
Length of cheektooth row (p3-m1)		36.1		31.0	37–38.5	37.0–37.1	37.2
Mandible depth in front of p3		18.7			17.1–21.5		19.1
Mandibular depth behind m1		20.3			19.1–26.5		20.9
Thickness of mandible under m1		9.4			8–10.2		9.3
TD of condyle		>15.9					21.0

exists the first order vascular pit (or nutrient foramen), which is similar to that in the extant *A. jubatus*. A small pointed coracoid process occurs on the robust supraglenoid tubercle, and it is hook-like and projects medially. In ventral view, the outline of the glenoid cavity is generally roundish but with an expanded sharp angle under the supraglenoid tubercle, which makes the anteroposterior diameter larger than the transverse one; the glenoid notch is not prominent (Fig. 4: 1B). The W/L index of the scapula is 53% (Table 3), which makes the overall appearance of the scapula more similar to that of canine than to feline (Roşu et al., 2016).

Radius: A complete left radius (V 31918.1) is preserved (Fig. 4: 3A-3D). The radius is quite slender but with expanded extremities, the shaft is fairly compressed anteroposteriorly, and with the middle portion convex cranially and medially, which looks rib-like. The proximal articular facet or glenoid fossa is kidney-shaped and quite depressed, and the medial portion is sloped downward and confluent with the surface of the medial coronoid process of the ulna. The articular circumference, a smooth band, occurs at the caudal aspect of the radial head, which contacts with the radial notch of the ulna. The radial (=bicipital) tuberosity is pronounced and has an vertically elongated oval surface, which is located at the posteromedial surface near the radial head. The nutrient foramen is located not far below the radial tuberosity. The distal end flares moderately; the radial styloid process is strongly developed and looks pointed in anterior view, the dorsal tubercle is also quite promounced but narrow; on the medial aspect, there exists a bladed crest (suprastyloid process) just above the styloid process; on the lateral aspect, there is no ulnar notch, but a distinct and smooth oval-shaped ulnar facet; along the lateral border of the whole body, there exists a nearly continued rugose belt; the distal articular facet only articulates with scapholunar, and it is a depressed oval surface whose long axis extends lateromedially, and the medial part has smaller diameter. The total length is 263, the proximal TD is 27.2, the proximal APD is 18.8, the distal TD is 42.2, the distal APD is 26.9, the L × W of the proximal glenoid fossa is 23 × 17. The radius is slightly longer than the extant *Acinonyx jubatus* whose length is 256 (Roşu et al., 2016); the dimensions are slightly less than those of *Acinonyx pardinensis* from Dmanisi, which is 271.4 long (Hemmer et al., 2011).

The highly projected but narrow dorsal tubercle and the anteroposteriorly compressed distal extremity are very similar to the characters of cheetah (*Acinonyx jubatus*) (Yalden, 1970).

Ulna: Only the proximal half of a left ulna remains, but it is well preserved (Fig. 4: 2). The olecranon process (or tuber) is robust and lateromedially compressed, and there is a groove between medial and lateral tubercles at the upper anterior part. The anconeal process is moderately developed. The medial coronoid process is much more robust than the lateral one. Both the sigmoid (or trochlear) notch and the radial notch are semilunar-shaped. The shaft is also compressed, but lateromedially. Olecranon process length (or height) is 52.0; smallest APD of olecranon is 34.0; depth across the anconeal process is 40.0; breadth across the coronoid process is 33.2.

This laterally positioned radial notch has been shown to be a consistent character within modern felids (Gonyea, 1978), contrasting with the more cranially located notch in canids and hyaenids (Rothwell, 2001). Furthermore, the tubercles on the olecranon process show great differences in size and shape within the Carnivora, and even among the Felinae, in the extant cheetah, as well as in canids, and the lateral tubercle has less proximo-distal development than the medial one (Salesa et al., 2010); the tubercles on the olecranon process of SSMZ specimen are very similar to that of the *Acinonyx jubatus* (Salesa et al., 2010, Fig. 8).

Although the partial ulna was not unearthed from the same horizon as the aforementioned radius (V 31918.2), they are very probably from the same individual.

Manus: An almost completely preserved left manus was unearthed, which includes all of the carpals and metacarpals as well as most of the finger bones (Fig. 4: 4).

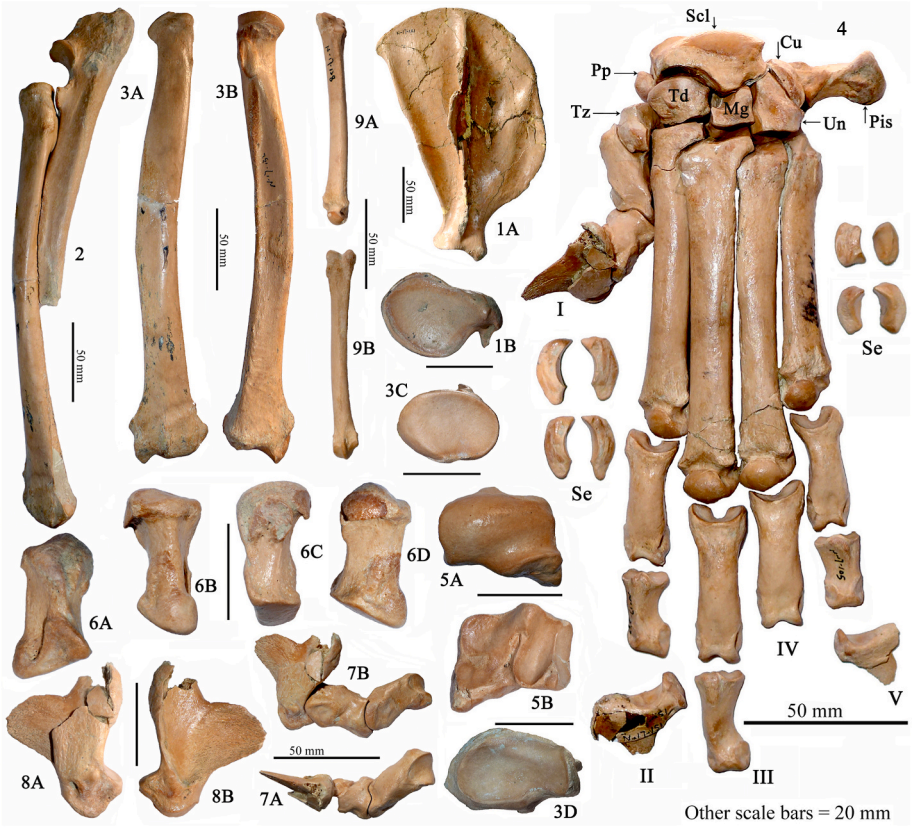

Fig. 4. *Acinonyx* sp. from SSMZ
1A-1B – right scapula (V 31918.1); 2 – left radius (V 31918.2) and left ulna (lacking distal part) (V 31918.3); 3A-3C – left radius (V 31918.2); 4 – left manus (V 31918.4–36); 5A-5B – details of the scapholunar (V 31918.5); 6A-6D – details of the pisiform (V 31918.7); 7A-7B – details of digit I (V 31918.13, 14, 20); 8A-8B – details of the distal phalanx of digit I or dewclaw (V 31918.26); 9A-9B – right Mt V
1A, 8B – lateral views; 1B, 3D and 5B – distal views; 2 – antero-lateral view; 3A – antero-medial view; 3B – posterior view; 3C and 5A – proximal views; 4, 6C and 9A – anterior views; 7A – dorsal view; 6A – radial (or superior) view; 6B and 9B – posterior views; 6D – ventral (or inferior) view; 7B and 8A – medial views.

Table 3
Measurements of scapula of *Acinonyx* sp. from SSMZ (in: mm).

Dimensions	SSMZ	*A. jubatus*	*A. pardinensis pleistocaenicus*
	This paper	Roşu et al. (2016)	Hemmer and Kahlke (2022)
Greatest length (from the superior border to the lower margin of the glenoid fossa)	220	203	226–232
Scapular spine length	185	183	
Greatest width, vertical to the spine	117	112	
Minimum width at the neck	34.7		44.1–44.9
Greatest length of the head	45.5		50–53.3
Smallest diameter of the head	29.7		
Anteroposterior diameter of the glenoid fossa	32		38.2–41.0
Transverse diameter of the glenoid fossa	28	27	30–32
Length of the coracoid process	>8	11	

Scapholunar (V 31918.5) (Fig. 4: 5A-5B): The scapholunar has a smooth convex and rectangle proximal surface, which closely matches the concave distal surface of the radius; on the other hand, the proximal surface also has a marked groove along the base of the posteromedial tubercle. The tip of the tubercle points to the inferior and medial direction. The distal surface of the scapholunar consists of four facets which articulate with the trapezium, trapezoid and magnum and unciform respectively; the trapezium and trapezoid facets are confluent and broadly concave, but the magnum facet is a separate narrow longitudinal groove; the boundaries of the magnum and unciform facets are nearly parallel to each other, which is a distinctive character of *Acinonyx* (Yalden, 1970); between the trapezoid and magnum facets, there is a beak-like projection at the anterior or dorsal aspect. Proximal surface TD is 29.7; proximal surface length is 17.8; posterior tubercle length is 18.3.

Cuneiform: It is a slice-like bone with the medio-lateral diameter greatly compressed. The median facet contacts unciform, lateral facet contacts ulna and pisiform respectively, distal facet contacts Mc V. The mediolateral width is 6.5; proximo-distal height is 13.8.

Pisiform (Fig. 4: 6A-6D): In this stick-like bone, the head is mushroom-like. The superior facet is confluent with the ulnar facet of cuneiform, and both of them contact the styloid process of ulna; the distal facet is quite flat and semicircular-shaped, which contacts cuneiform. The tubercle width is 13.3; total length is 28.6.

Trapezium: It is an irregular-shaped bone. The superior or largest facet contacts scapholunar; the medial facet is semilunar-like and articulates with Mc I; the two lateral facets contact trapezoid (upper) and Mc II (lower) respectively. The anteroposterior length is 15.2; proximodistal height is 13.2.

Trapezoid: In dorsal view, the proximal and distal margins are nearly parallel; in proximal view, the scapholunar facet is belt-like and convex; in medial view, the facet for trapezium is quite flat; in lateral view, the magnum facet is not prominent. The mediolateral width is 17.6; proximodistal height is 11.0.

Magnum: It is an irregular-shaped bone. In proximal view, a pronouncedly arched and anteroposteriorly oriented narrow facet can be seen, which contacts scapholunar; in distal view, the facets for Mc II-IV can be seen; in medial view, the facets for Mc II, Mc III, trapezoid and scapholunar can be seen, among which the facet for Mc III is the largest; in lateral view, only the scapholunar and unciform facets can be seen. The anteroposterior length is 24.3; proximodistal height is 15.3.

Unciform: In proximal view, the pronouncedly arched and anteroposteriorly oriented narrow scapholunar facet can be seen; in distal view, the large concave facets for Mc IV and Mc V are confluent; in medial view, the magnum facet can be seen, which is divided into the upper and lower parts; in lateral view, only the cuneiform facet can be seen. The anteroposterior length is 20.6; proximodistal height is 18.2; medio-lateral width is 13.5.

The Mc I (Fig. 4: 7A-7B; Table 4) is the most peculiar one among the metacarpals, whose general form resembles that of a leopard (Salesa et al., 2010, Fig. 14), but much slenderer and with the proximal and distal articular facets very steep, also much more concave; the proximal facet can only be seen in dorsal view, while the distal facet can only be observed in plantar view. The blade-like palmar keel of the distal articulation is well developed.

Other metacarpals (Mc II-V) are similar in having much longer shaft (Fig. 4: 4) and spherical metacarpal head (distal articulate facet) as well as robust and long median keel; but none of them shares the same proximal facet with others.

Mc II is longer than Mc I and Mc V, but shorter than Mc III and Mc IV; the proximal facet of Mc II is relatively higher positioned than others. In medial view, the facet for trapezium is clear enough, but there is no prominent facet for Mc I. In proximal view, the facet for trapezoid is triangular. Mc II partially overlaps Mc III at the proximal end. The two lateral facets contact magnum and Mc III respectively (Fig. 4; Table 4).

Mc III is the longest metacarpal. The two proximal facets contact the magnum and Mc II respectively. The two lateral facets contact the unciform and Mc IV respectively. Mc III partially overlaps Mc IV at the proximal end (Fig. 4; Table 4).

Mc IV is longer than others except the Mc III. The two proximal facets contact the unciform and Mc III respectively. The lateral facet contacts the Mc V (Fig. 4; Table 4).

Mc V is shorter than others except Mc I. The narrow proximal facet is for unciform, and the medial facet is for Mc IV. The shaft is slightly concave to the medial direction (Fig. 4; Table 4).

The proximal phalanx of the thumb is the most robust and also the shortest proximal phalanx; both the proximal and distal facets are asymmetrical. The other four proximal phalanges have approximately symmetrical proximal and distal facets; the proximal facets are deeply concave, and there is a prominent and deep posterior notch, which matches the median keel of the metacarpal; the distal articular facet is divided by a sagittal groove; all of the proximal phalanges, except that of digit I, are relatively longer than those of the middle phalanges, and their shafts are dorsally bowed.

The digits II-V have the middle phalanges which are much smaller than the proximal ones; the proximal articular facet is divided into two smaller concave subfacets by a sagittal ridge, but the proximoposterior notch is replaced by a deep pit; they are expanded at the lateral portion of the distal end (with lateral asymmetry), which means the mid-shafts usually have their lateral edges much more concaved than the medial side (Fig. 4; Table 4), but not bowed dorsally.

Concerning the phalanges, it is almost impossible to distinguish the manus phalanges from those of the pes (Merriam and Stock, 1932). The SSMZ cheetah phalanges maybe a mixture of both manus and pes, and the phalanges of the pes should have more roundish cross-section of the body (or shaft) and roundish proximal facet.

The distal (or third or ungual) phalanges are very peculiar in felids, because their bony part is usually higher (or deeper) than long and strongly compressed mediolaterally. The unguicular hood is moderately developed, lesser than in pantherines but stronger than that of modern *Acinonyx*; the claw core or unguicular process is not so pointed (Fig. 4: 8B) as in pantherines (Cueto et al., 2016) and *Felis* (Homberger et al., 2009); the articular facet is less concaved; the plantar process or flexor tubercle is stout. The principal vascular (or subungual) foramen is quite big, which occurs at the lateral side of the plantar process. The measuring method of the ungual phalanx of this paper is different from that used by Salesa et al. (2010), and we define the height as the vertical distance between the superior border of the unguicular hood and the inferior border of the plantar process (Table 4).

The metatarsal V (V 31918.37) is quite slender; its greatest length is 111.2. The shaft is curved and compressed dorsoventrally. There are two proximal articular facets which contact cuboid and Mt IV respectively; both of them are located at the medioanterior aspect. The distal articular facet is asymmetric, and the lateral portion is fairly reduced. The median keel is pronounced (Fig. 4: 9A-9B). The Mt V length of SSMZ specimen is longer than those of *Smilodon californicus* (70.8–94.8) (Merriam and

Table 4
Measurements (in: mm) of metacarpal and phalangeal bones of *Acinonyx* sp. from SSMZ.

Metacarpals	Digit I	Digit II			Digit III			Digit IV			Digit V		
	Mc. I	Mc. II			Mc. III			Mc. IV			Mc. V		
	SSMZ	SSMZ	DMN	UMF	SSMZ	DMN	UMF	SSMZ	DMN	UMF	SSMZ	DMN	UMF
Greatest length	30.7	89.2	95.3	104.3	104.5	109.2	113.5–123.1	99.4	106.9	103.0–119.4	79.7	86.3	92.0–95.0
Maximal proximal TD	13.5	15.3	19.8	19.2	18.3	22.0	20.8–21.0	12.0	13.7	15.5	9.6	15.5	18.0
Maximal proximal ADP	11.2	20.7	23.5	25.0	17.2	20.5	21.0–21.1	16.6	20.4	18.9	13.8	18.2	18.0
Minimal shaft TD	10.7	8.5	10.7	12.5	10.0	12.8	13.0–15.0	8.2	11.3	11.0–12.6	9.0	9.8	10.0–11.5
Minimal shaft APD	8.2	11.1			8.3			9.2			7.1		
Maximal distal TD	10.3	14.3	16.7	18.7	16.9	17.8	20.0–20.1	15.3	16.8	17.9	14.3	16.5	17.5
Proximal phalanx													
Length of proximal phalanx	22.8	37.5			44.8			41.0			34.1		
Maximal proximal TD of proximal phalanx	14.4	13.9			15.2			14.6			13.8		
Maximal proximal APD of proximal phalanx	11.3	12.0			12.1			11.9			11.3		
Maximal distal TD of proximal phalanx	13.4	12.0			12.1			12.3			11.3		
Middle phalanx													
Length of middle phalanx		25.6			31.0						21.2		
Maximal proximal TD of middle phalanx		12.0			13.2						11.4		
Maximal proximal APD of middle phalanx		11.5			11.3						10.5		
Maximal distal TD of middle phalanx		11.3			11.3						9.6		
Distal phalanx													
Height of distal phalanx	>35.1	>29.0									>18.0		
Maximal TD of distal phalanx	>12	>9.0									>7.0		
Maximal APD of distal phalanx	26.6	21.0									18.0		

Data sources: DMN (Hemmer et al., 2011); UMF (Hemmer and Kahlke, 2022).

Stock, 1932), but shorter than those of *A. pardinensis* (116.7 by Van Valkenburgh et al., 1990 and 129 by Hemmer, 2001); moreover, it's extraordinarily close to that of the extant tiger *P. tigris* (108.5–110.8) (Baryshnikov, 2016).

Comparisons and discussions: The current taxonomic scenario divides the family Felidae into 2 subfamilies (Pantherinae and Felinae) and 8 lineages, and the cheetahs are assigned to the puma lineage (including *Puma concolor*, *Herpailurus yagouaroundi*, and *Acinonyx jubatus*) under Felinae (Kitchener et al., 2017). Whereas other researchers referred cheetahs to the subfamily Acinonychinae Pocock, 1917 (McKenna and Bell, 1997). The present authors also support the assignment of cheetahs to Acinonychinae, because the body size and body mass of the animals of the puma lineage are outstandingly larger than those of other taxa of the subfamily felinae (Mattern and McLennan, 2000).

Among the large felids, the SSMZ specimens resemble the extant cheetah very much in morphology, especially in scapula, radius, scapholunar and phalanges, but slightly larger in size. Furthermore, the SSMZ dewclaws and other ungual phalanges are much more developed, and the distal end of the middle phalanges exhibit stronger lateral asymmetry.

The SSMZ scapula looks like that of *Acinonyx jubatus* in its narrower and rectangular shape, which is different from that of leopard whose scapula is broader and more fan-shaped in order to enhance climbing (Sreeranjini and Ashok, 2008; Kitchener et al., 2010: Fig. 3.4). On the other hand, the SSMZ scapula is prominently larger than those of leopards whose scapula length ranges are 123.2–150.8 for females and 144.6–170.3 for males respectively (Christiansen and Adolfssen, 2007). Although the SSMZ scapula shares almost the same size as that of *Megantereon cultridens* from Senéze whose dorso-ventral length is 217.8–221.6 (Christiansen and Adolfssen, 2007), but the latter's neck is shorter. The SSMZ specimen is smaller than those of *A. pardinensis pleistocaenicus* from Untermassfeld (Hemmer and Kahlke, 2022).

Among the forelimbs of cheetahs, the radius account for the largest proportion (38.8 ± 1.2%), which is almost the highest among the felids; cheetahs have relatively long limbs for their mass but not for their body length (Day and Jayne, 2007). Cheetahs' forelimbs are modified to be distally elongated with a long radius and ulna, relative to humerus (Meachen et al., 2018). The SSMZ radius is much longer than those of the *Megantereon cultridens* from Senéze whose overall length is 216.2–220.7 (Christiansen and Adolfssen, 2007) and those of *Panthera pardus* from Equi site (182–211.6) in Italy (Ghezzo and Rook, 2015); and the form is also different from that of the extant leopard in its relatively pronounced radial tuberosity (Sreeranjini et al., 2014) and strongly compressed shaft (Ghezzo and Rook, 2015) as well as a more upper and volarward position of the radial tuberosity (Hopwood, 1947). The SSMZ radius is prominently smaller than that of a female *Panthera leo spelaea* whose radius length is 288 (Diedrich, 2011). The dimensions of the SSMZ scapula and radius are also smaller than those of extant *Panthera leo* (Sohel et al., 2021). The SSMZ radius is very similar to the counterpart of *Acinonyx pardinensis* from Dmanisi, whose length is 266 (Hemmer et al., 2011); while it is much longer than that of an extant *Acinonyx jubatus*, whose radial length is 222.3 (van Valkenburgh et al., 1990).

The scapholunar resembles that of extant *Acinonyx jubatus* in morphology. Previous studies have shown the difference between cheetah and pantherine taxa in the distal surface of scapholunar, which has the groove and ridge sub-parallel and less distinct (Hopwood, 1947).

The Mc III of SSMZ specimen is longer than that of the extant *Acinonyx jubatus* whose length is 88.4 (van Valkenburgh et al., 1990), but slightly shorter than those of *Acinonyx pardinensis* from Dmanisi (Hemmer et al., 2011). All the metacarpal bones are shorter and slender than those of *Pachycrocuta brevirostris* from Untermassfeld (Iannucci et al., 2022).

The Mt. V is slightly shorter than that of *Acinonyx pardinensis* whose Mt. V length is 116.7 (van Valkenburgh et al., 1990), and very close to that of *Panthera gombaszogensis*, whose Mt V length is 101.4 (Argant and Argant, 2011). Comparing with the *Panthera tigris* (Mt. V length is 110.7) from Salawusu, the SSMZ specimen is slightly longer but much slender.

Moreover, the metapodials of SSMZ specimens of *Acinonyx* sp. are much longer than the counterparts of *Panthera pardus* (Ghezzo and Rook, 2015) and those of *Megantereon cultridens* from Senéze (Christiansen and Adolfssen, 2007).

The modern cheetah *Acinonyx jubatus* is an atypical felid, well known for having blunt, only slightly curved, and partially retractile (semi-retractable) claws (Pocock, 1917; Gonyea and Ashworth, 1975; Londei, 2000; Russell and Bryant, 2001); while it has a very large, recurved and sharp claw of the first digit of the forepaw, the so-called dewclaws, which are used to snag and pull preys off balance, and which are different from other pantherine (tigers, lions and leopards), who rely on a strong impact instead to strike the prey to the ground (Londei, 2000; Kitchener et al., 2010). Among the large-sized felids, cheetah has much stronger dewclaw relative to its second-digit claw, i.e. with a higher claw ratio (Londei, 2000). However, the dewclaw of modern cheetah seems have much more reduced hood (Antón et al., 2005: Fig. 6) relative to the SSMZ specimens, which have well developed ungual phalanges, not only for the first digit, which is a crucial character to distinguish it from the extant cheetah. It is worth mentioning that the Mc I is extremely short relative to its Mc II (Table 4) in the SSMZ specimen.

In sum, the postcranial bones of *Acinonyx* sp. from SSMZ are slightly smaller than those of *Acinonyx pardinensis* from Dmanisi (Hemmer et al., 2011) and are prominently smaller than those of *A. pardinensis pleistocaenicus* from the Untermassfeld site (Hemmer and Kahlke, 2022) and Saint-Vallier (Argant, 2004); but are much slender than those of *Panthera tigris, Panthera leo,* and even *Pachycrocuta.* Although hyaenids also have slender limb bones as cheetahs do (Martín-Serra et al., 2014), the former has a vestigial dewclaw (Senter and Moch, 2015), rather than lacks the Mc I as known before; furthermore, the ungual phalanx of cheetah is completely different from that of a hyena. Therefore, the SSMZ manus bones have little in common with hyena.

All of the *Acinonyx* fossils from SSMZ very probably belong to the same individual, although they scattered in different grids and horizons in the geological context (see Table 1).

Although Pei (1987) suggested that all of the Chinese Pleistocene cheetah fossils should be grouped under the same species, *Cynailurus pleistocaenicus*) or *Acinonyx pardinensis*, as suggested by European researchers (Cherin et al., 2014b), it is helpful to give an overview of the crucial taxa and localities ever reported in China. The important taxa and localities of the Early Pleistocene cheetahs are as follows: *Cynailurus* (=*Acinonyx*) *pleistocaenicus* from Yuanqu (Yüan-Chü) in Shanxi (Zdansky, 1925); *Cynailurus pleistocaenicus* from Xiashagou in Hebei (Teilhard de Chardin and Piveteau, 1930); *Sivapanthera pleistocaenicus* from Gongwangling in Shaanxi (Hu and Qi, 1978); *Cynailurus* (*Acinonyx*) *pleistocaenicus* from *Gigantopithecus* Cave in Guangxi (Pei, 1987); *Sivapanthera linxiaensis* from Longdan in Gansu (Qiu et al., 2004); *Acinonyx pleistocaenicus* from Jianshi in Hubei (Zhang and Feng, 2004); *Acinonyx arvernensis* from Tuozidong in Jiangsu (Liu et al., 2007); *Acinonyx* sp. from Shigou in Nihewan (Chen et al., 2017). The cranial and dental characters of the specimens from Tuozidong have very high similarity to those of the extant species *Acinonyx jubatus* except its larger size. The specimen from Xiashagou also resembles that of the extant *Acinonyx jubatus* in form but slightly larger in size. The mandible specimen from Gongwangling has an overdeveloped talonid on m1 and the conical principal cuspids as well as robust cusplets on lower premolars; in addition, its W/L ratio of the teeth is also prominently larger than those of other Early Pleistocene cheetahs; the specimens from Longdan and Yangshuizhan in Nihewan are prominently different from the extant *Acinonyx jubatus* in their less domed but much more elongated crania; moreover, they substantially resemble the European *Acinonyx pardinensis*. The Middle Pleistocene cheetahs only scarcely appeared at ZKD Loc. 1 and 13 as *Cynailurus* sp. (Pei, 1934; Teilhard de Chardin and Pei, 1941) and Jinniushan site as *Acinonyx* cf. *jubatus* (Zheng and Han,

1993). The Late Pleistocene cheetah (*Cynailurus* cf. *jubatus*) was fairly well represented at the Upper Cave in Zhoukoudian, and the fossils include an entire skeleton with skull and mandible (Pei, 1934, 1940). Unfortunately, the fossil materials are presumably lost before they can be studied; the only P4 examined shows that the Late Pleistocene cheetah of Upper Cave was still larger than the extant Indian cheetah (Pei, 1940). As early as 1941, Teilhard de Chardin and Pei had noticed the gradual diminution of the cheetahs' size since Early Pleistocene onward. The fossil cheetahs of North China were once divided into two groups: the larger one from Yuanqu and the smaller one from Nihewan, and only the small one survived into Mid-Late Pleistocene (Pei, 1987).

In China, although fossil cheetahs were poorly represented (Tong et al., 2011b), they did exist throughout the entire period of Pleistocene, and even can be traced back to late Neogene (Qiu et al., 2013). Based on the forms and dimensions of the upper and lower carnassial teeth, it seems that the scatter plot of P4 is quite regular and linear, except in few abnormal samples (Fig. 5: A). The data points for m1, on the other hand, are not well clustered (Fig. 5: B), which suggests that either the m1s are more variable in size or the identifications of the specimens are questionable. It is very probable that they were a mixture of cheetahs with the *Panthera* species. The maxillary and mandibular fragments of *Sivapanthera pleistocaenicus* from Hexian are prominently larger than others; furthermore, the P3 has a rather small and lingually located anterior accessory cusp, and P4 has a robust and anteriorly located protocone, which makes the width obviously larger than a cheetah's tooth, and the p3 has weak accessory cusps. The above mentioned traits are never or very rare in cheetahs; the Hexian record is very probably not a *Sivapanthera pleistocaenicus*. One of the upper P4 from Liucheng *Gigantopithecus* Cave is also extraordinarily larger than others, and was provisionally referred to cheetah. Furthermore, the Middle and Late Pleistocene specimens stand between those of the Early Pleistocene and the extant form, which means the cheetah lineage did undergo a decline in body size through its evolution. Even though all of the Chinese fossil cheetahs are larger than the extant species, they are more closely related to them than to the European ones in both form and size.

In Nihewan Basin, two kinds of cheetah-like carnivores have been recognized: the modern cheetah sized which is identified as *Acinonyx* sp., and the giant cheetah sized which should belong to *Acinonyx pleistocaenicus*. The specimens of the former include the mandible from XSG (Teilhard de Chardin and Piveteau, 1930), and the partial skull from Shigou (Chen et al., 2017) as well as the postcranial skeletons described in this study; the latter includes a nearly complete skull recently unearthed from Yangshuizhan (unpublished). Both the small one and the larger one have short canines and reduced protocone on P4. It is very possible that there were two kinds of cheetah once living in Nihewan Basin during the Early Pleistocene epoch, one is the primitive, *Sivapanthera*-like form, which has elongated and less domed cranium, and the other is the *Acinonyx*-like which is slightly smaller and with domed cranium. The smaller form of Cheetah from XSG is obviously smaller, and the dimensions of its lower teeth (IVPP RV30006) are as follows: p3 L × W = 14.3 × 6.6, p4 L × W = 19.0 × 7.5, m1 L × W = 20.0 × 7.6 (the datum of m1 length is from Teilhard de Chardin and Piveteau, 1930).

In general, the cheetah-like fossils from Nihewan are closer to the extant cheetah in its size and form of the P4 which has reduced protocone and prominent preparastyle or ectoparastyle. Christiansen and Mazák (2009) indicated that one of the most peculiar features of the cheetah's upper carnassial is the presence of a well-developed ectoparastyle (this paper was retracted in 2012). Meanwhile, Cherin et al. (2014b) proposed that although the extant *A. jubatus* is characterized by a prominent ectoparastyle, it cannot be considered a diagnostic character; in fact, it is also present in such large felids as *Panthera onca* and *P. tigris*, and shows a remarkable individual variability. Therefore, the recognition of *Panthera*-like characters in *A. pardinensis* leads to the reconsideration of its ecological role, which should be different from those of the living cheetah. Furthermore, the high intraspecific variations in body size in *A. pardinensis* may be resulted from sexual dimorphism.

The Early Pleistocene giant cheetah species, *Acinonyx pleistocaenicus* and *Sivapanthera linxiaensis*, have the same skull characters and similar size with those of European giant cheetah *Acinonyx pardinensis*, except the late Early Pleistocene Untermassfeld specimens; while the smaller fossil cheetahs, *Acinonyx* sp. (including the *Acinonyx arvernensis* from Tuozidong) from China stands between the giant cheetah and the extant form both in characters and in size. Recently, Cherin et al. (2014b) revised the taxonomy of the old-world fossil cheetahs, in which, they grouped almost all of the Early Pleistocene fossil cheetahs from China into the species *Acinonyx pardinensis*, but not including the *Acinonyx* sp. from XSG of Nihewan. Spassov (2011) also grouped all the fossil cheetahs of Europe under one species but at different subspecies or chronoforms: *A. pardinensis pardinensis*, *A. p. pleistocaenicus* and *A. p. intermedius* in a succession from the Early Villafranchian (Etouaires, approx. 2.6 Ma) till the Middle Pleistocene. A recent study on the fossils of *A. pardinensis* from Monte Argentario of Italy reveals a mosaic of cheetah-like and *Panthera*-like features (Cherin et al., 2018). Morphological comparisons and morphometric analysis of the fossil and recent material show that the *Acinonyx pardinensis* from Saint-Vallier, although dentally similar to the modern cheetah, is not cheetah-like in its skull shape, and the characteristic skull shape of the modern cheetah is probably a recent acquisition (Geraads, 2014).

The richest fossil collection of *A. pardinensis pleistocaenicus* is from

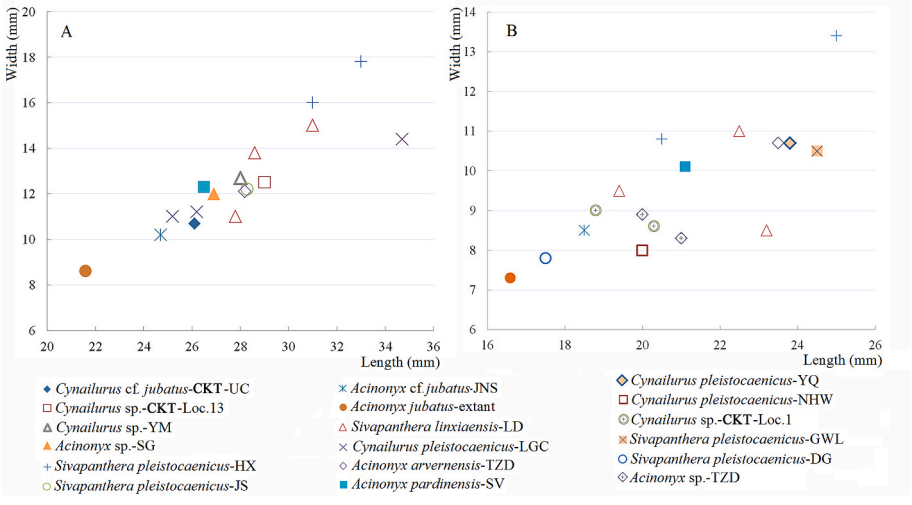

Fig. 5. L × D of upper P4 (A) and lower m1 (B) of diverse fossil cheetahs of Pleistocene age from China.

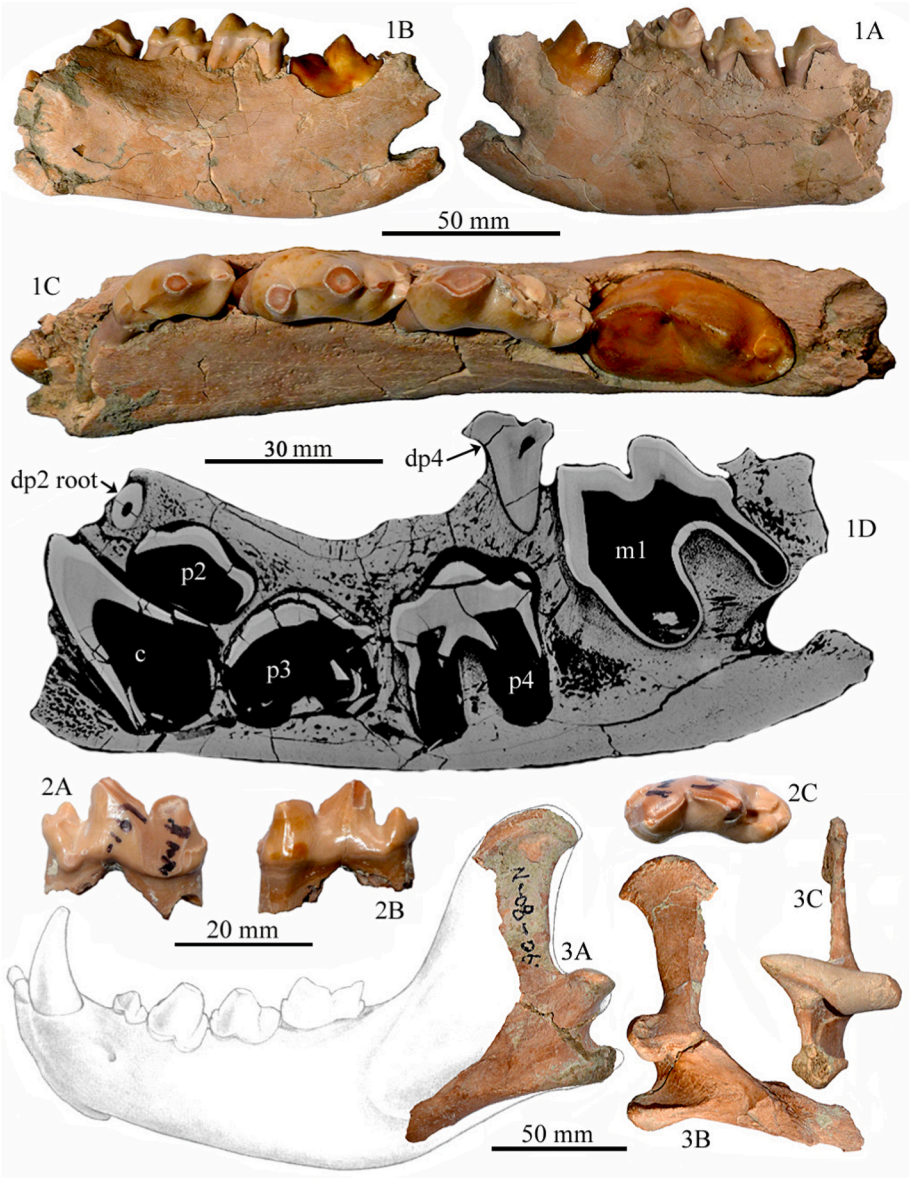

Fig. 6. *Pachycrocuta licenti* from SSMZ
1A-1D – partial right mandible with dp2-4 and m1 (V 31920); 2A-2C – isolated right dp4 (V 31921); 3A-3C – partial mandible with broken ramus and condyle as well as angular process (V 31922). The mandible outline as background in Fig. 6: 3A is after Werdelin and Solounias (1991: Fig. 4), horizontally flipped.

Untermassfeld of Germany, which includes skulls, mandibles and a large quantity of postcranial bones (Hemmer and Kahlke, 2022) and are prominently larger than the SSMZ specimens (Table 4).

It was once proposed that cheetahs originated in the North American puma lineage and migrated to central Asia and Africa (Johnson et al., 2006), and quite a number of studies also group *Puma* with *Acinonyx* (Johnson et al., 2006; Bellani, 2020). Comparisons between the puma (*Puma concolor*) and the cheetah (*Acinonyx jubatus*) show that the latter has shorter, deeper and more domed skull, broader frontal, palatine and choana fossa, higher crown but gracile teeth, more reduced protocone of P4, shorter mandibular symphysis. Van Valkenburgh et al. (1990) also shows that the latter has a more gracile body build. It seems that the extinct puma-like cats (*Miracinonyx inexpectatus* and *M. trumani*) of North America are also less related with those of the old world cheetahs. Van Valkenburgh et al. (1990) recognized distinctions between old world *Acinonyx* and the American *Miracinonyx*. Subsequent phylogenetic analyses reveal that *M. trumani* is the sister taxon to the puma, rather than the African cheetah (Barnett et al., 2005). In spite of the similarities between *M. trumani* and *Acinonyx*, it was regarded as an example of parallelism rather than common origin; because many of the muscle scars and details of the skull and skeletal anatomy suggest that *Miracinonyx* may be more closely related to the puma than to cheetah (Martin et al., 1977). The fossil record suggests that cheetahs originated in Africa as *Acinonyx* sp. at about 3.85–3.60 Ma (Werdelin and Dehghani, 2011; Cherin et al., 2014b) or ~4.0–3.0 Ma (Van Valkenburgh et al., 2018). Subsequently its relative, *Sivapanthera* sp. appeared in the Mazegou land mammal stage (3.7–2.9 Ma) of Yushe Basin in North China (Qiu et al., 2013), while the earliest fossil record of the most cheetah-like skull was recovered in China, i.e., *Acinonyx arvernensis* from Tuozidong (Liu et al., 2007). The 'giant' cheetah *A. pardinensis* appeared in western Europe a little over 3 Ma (Werdelin et al., 2010). In central Asia, the occurrence of *Acinonyx* ex. gr. *pardinensis* can be trace back to the MN16 (Sotnikova et al., 1997); while in South Asia, no definite fossil record was reported. Although the living species, *A. jubatus*, appeared first in southern Africa at ~1.9–1.8 Ma (Van Valkenburgh et al., 2018), China is one of the most important evolutionary centers for early

cheetahs.

Subfamily Machairodontinae (Gill,1872) Hay, 1930
Genus *Homotherium* Fabrini, 1890

***Homotherium* sp.**

(Fig. 3: 4A-4C).

?*Megantereon nihowanensis*, Tong et al., 2021, p. 481.

Material: paraconid blade of a left m1 (V 31919).

Descriptions:

The partial m1 (Fig. 3: 4A-4C)**:** The paraconid or anterior blade is quite robust. At the anterobuccal aspect, there exists a vertical groove, which indicates the vestigial front-lobe (Pei, 1934) and should be a character of the *Homotherium* m1 (see Pei, 1934: Pl. XXII-5b). The lingual aspect is buccally concaved and some tiny enamel tubercles occur in the valley (Fig. 3: 4C). The root is moderately developed and its length is approximately 19, which is much shorter than that of *Panthera tigris* (Tong et al., 2019); furthermore, the root is fairly compressed linguobuccally and rapidly tapered toward the apex. The protoconid or the posterior blade was broken off. The wear facet of the m1 has a typical machairodontine form, which is usually much more deeply extended downward at the buccal aspect, and even reaches the dental cervix; furthermore, the wear facet often have vertical grooves or striae (Fig. 3: 4A). The least width (bucco-lingual diameter) is 12.7.

Comparisons and discussions: The wear facet and root morphology are quite different from those of Pantherines. Both *Homotherium* and *Megantereon* have been recognized in the CNF (or Xiashagou fauna) (Qiu et al., 2004). In shape, the partial m1 from SSMZ is similar to those of *Homotherium* from Zhoukoudian (Pei, 1934) and Renzidong (Liu and Qiu, 2009) as well as Jianshi (Zhang and Feng, 2004). The bucco-lingual dimension is 12.7, which is very similar to those of *Homotherium* sp. from ZKD Loc.1 (Pei, 1934) and from Jianshi (Zhang and Feng, 2004) as well as *Homotherium latidens* from Alaska and Iberian Peninsula (Antón et al., 2014). The partial m1 is larger than all of the m1s of *Megantereon* species ever reported, including those from Longdan (Qiu et al., 2004); moreover, it is much smaller than that of *Panthera tigris* (Pei, 1934; Tong et al., 2019). It is worth mentioning that the root of the m1 from Renzidong is extraordinarily slender and more pointed than usual.

Moreover, the dimensions of the partial m1 fall within the ranges of *Homotherium* spp., and the wear facet is also similar to that of *Homotherium* (Sardella and Iurino, 2012).

The most recent study on a nearly complete skull of *Homotherium crenatidens teilhardipiveteaui* from Nihewan shows that body size cannot be used as a determinate trait for species/subspecies delimitation; on the other hand, the crown height of the upper canine shows a decrease at the early/middle Early Pleistocene boundary ~1.8 Ma (Jiangzuo et al., 2022a,b,c).

Family Hyaenidae Grey, 1821
Subfamily Hyaeninae (Grey,1821) Mivart, 1882
Genus *Pachycrocuta* Kretzoi, 1938

***Pachycrocuta licenti* (Pei, 1934).**

(Fig. 6; Tables 5 and 6).

Hyaena sinensis, Teilhard de Chardin and Piveteau, 1930, pp. 101-104.

Hyaena licenti, Pei, 1934, pp. 120-121.

?*Panthera* sp., Tong et al., 2021, p. 481.

Materials: Partial right mandible with dp2–4 and m1 (V 31920), isolated right dp4 (V 31921), partial mandible with broken ramus and condyle as well as angular process (V 31922).

Descriptions.

A partial mandibular body with the dp2–4 and m1 as well as the erupting canine preserved in situ (Fig. 6: 1A-1C) and p2–4 are still in alveolus (Fig. 6: 1D). Each of the lower cheek teeth, both deciduous and permanent, has two roots (Table 5).

Table 5
Dimensions of the lower teeth of *Pachycrocuta licenti* from SSMZ, compared with related taxa.

		Pachycrocuta licenti		*Pachycrocuta brevirostris licenti*	*Pachycrocuta perrieri*	*Pachycrocuta sinensis*	*Pachycrocuta sinensis*	*Crocuta honanensis*	*Crocuta crocuta spelaea*	*Crocuta crocuta spelaea*	*C. ultima ussurica*	*Crocuta crocuta crocuta*	*Hyaena hyaena*	*Crocuta ultima*	*Panthera tigris*
		V 31922	V 31921	Liu and Qiu (2009)	Argant (2004)	Tong et al. (2019)	Pei (1934)	Qiu et al. (2004)	Pappa et al. (2005)	Baryshnikov (2014)	Baryshnikov (2014)	Kurtén (1956)	Kurtén (1956)	Kurtén (1956)	Baryshnikov (2016)
dp2	L	13.0			?8.0–13.3	15.0**	14.6–15.0			9.2**		8.6	11.8	10.2	
	W	6.3			6.9		8.0–8.2			5.0–5.1	5.0				
dp3	L	16.3			16.6	18.7**	18.2–18.4	13.1[a]	13.3–14.7	12.3–14.4	13.0	13.5	14.9	14.1	
	W	7.0			8.1		8.7–9.4		6.6–7.1	6.1–6.8	6.0				
dp4	L	19.0	20.0		19.8	20.0*	20.1–20.6	16.5[a]	18.1	18.9–21.9	18.8–21.8	17.9	17.1	20.0	15.6[b]–18.5[c]
	W	>6.4	7.3		7.9	7.2*	8.0–8.3		6.7–7.9	7.2–8.8	7.8–8.5				5.6[b]–7.2[c]
m1	L	27.3		27.4	29.7–30.4**	28.6–30.2	29.2–29.6	24.3–25.8		32.6**		26.7	20.78 ± 0.1	32.8	24.6
	W	13.0		14.9	14.3–15.4	14.9–15.5	15.0–16.3	10.9–11.6							12.4

* Measured by the first author of this paper.
** *P. brevirostris* (Iannucci et al., 2022).
[a] Calculated by the present author on the text-fig. 31 of Teilhard de Chardin and Piveteau (1930).
[b] Extant.
[c] Fossil.

The dp2 has only one principal cuspid (protoconid), and a moderately developed posterior cusplet, but there is no anterior cusplet.

The dp3 has the protoconid as the principal cuspid. The anterior accessary cuspid is also well developed, while the posterior accessary cuspid is relatively small; a talonid is extraordinarily well-developed.

The dp4 is buccolingually compressed, and the lingual aspect is concave buccally. The paraconid and protoconid are equally developed, but the latter is slightly higher. The carnassial notch extends downward not very deep; between the protoconid and the hypoconid there is a deep notch. The talonid is quite long, with the entoconid well-developed and hypoconulid moderately developed, but the hypoconid is vestigial, while the metaconid is completely absent.

The dp4 is characterized by its buccolingually compressed crown and very developed talonid with crest-like hypoconid and conical entoconid, which are quite similar to those of *Crocuta crocuta spelaea* (Pappa et al., 2005) and *Crocuta ultima ussurica* (Baryshnikov, 2014), but different from that of *Pachycrocuta sinensis*. The latter only has a central trenchant cuspid on the talonid which was identified as hypoconid (Pei, 1934).

The p2 (partially formed and unerupted) is prominently smaller than p3 and p4; with only one principal cuspid (protoconid) developed, and a moderately developed posterior cusplet, but there is no anterior cusplet.

The p3 (partially formed and unerupted) is enlarged relative to p2, but with nearly the same structure.

The p4 (partially formed and unerupted) is slightly larger than p3, but with both the anterior and posterior cusplets developed.

The m1 shows a typical form of *Pachycrocuta* in its unicuspid talonid according to Werdelin and Peigné (2010), with the carnassial blade (trigonid) elements (paraconid and protoconid) well developed, but the paraconid is prominently stronger (longer and wider) than the protoconid, while the latter being slightly higher. The metaconid is vestigial, being at a more buccal position and close to the hypoconid. The talonid is well developed, and with a distinct conical hypoconid which is located more lingually than usual (Fig. 6: 1C), entoconid is vestigial, and hypoconulid is absent. The posterior cingulum is faint.

An isolated dp4 is fairly well-preserved, with paraconid and protoconid equally developed, but the metaconid is absent, the talonid is composed of an entoconid and a less developed hypoconid as well as a tiny hypoconulid. The buccal wear facet extends quite far downward (Fig. 6: 2A-2C).

A partial mandibular ramus pereserves with the angular process, the condylar process and the summit of the coronoid process (Fig. 6: 3A-3C). The posterior border of the coronoid process, the condyle and the angular process are almost at a same straight line. The coronoid process is high with a superior rim at the buccal aspect, which is for insertion of the temporal muscle. The majority part of the masseteric fossa is broken off. The condyle is perfectly preserved, whose articular facet is fusiform with the lingual portion whirling downward; the superior border is not straight.

The angular process is moderately developed, and is posteroventrally and slightly medially directed, with a medial and an inferior crest; the superior surface is spoon-like; between the lingual crest and the condyle, there exists a trench that leads to the mandibular foramen; at the buccal aspect, a crest exists along the lower edge which derives from the angular process and extends 63.6 mm forward that represents the lower boundary of the masseteric fossa. The ramus height at coronoid process (from inferior border of angular process to summit of coronoid process) is 112.8 mm; the ramus height at condyle or distance from dorsal border of condyle to ventral border of angular process is 45.3 mm; the mediolateral diameter of the condyle is 55.3 mm.

Comparisons and discussions: In China, the deciduous teeth of *Pachycrocuta* are well represented in the fauna of ZKD Loc.1 (Pei, 1934). The dp4 of *Pachycrocuta sinensis* from there has large size, and its metaconid is absent and has only one talonid cuspid (hypoconid) (Pei, 1934), which are quite different from the SSMZ specimens. Moreover, the SSMZ dp4 shares the same characters with those of *P. licenti* from Jianshi Longgudong (Zhang and Feng, 2004). The dp4 of *Hyaena* sp. from XSG of Nihewan also has no metaconid (Teilhard de Chardin and Piveteau, 1930). Although the SSMZ dp4s have similar dimensions with those of *Smilodon*, the latter has larger metaconid and talonid cuspids, including two distinct lobes of the metastylid (Merriam and Stock, 1932). In *Homotherium serum*, the notch between the paraconid and metaconid is an open V in the dp4 and a closed V in the m1; in addition, the dp4 has a small metastylid behind the metaconid (Rawn-Schatzinger, 1983); the L × W of dp4 is 9.9 × 4.5 mm (Rawn-Schatzinger and Collins, 1981), which is prominently smaller than that of *P. licenti*.

Concerning the lower carnassial tooth, the teeth of *P. sinensis* normally has no metaconid, and the talonid is short and has only a distinct hypoconid (Pei, 1934). The *P. licenti* from Jianshi Longgudong have considerable variations both in dimensions and form; the length of m1 ranges from 26.4 to 31.5 and the mean value is 28.5; some of the m1s have both entoconid and hypoconid, while others only have hypoconid, but the metaconid is completely absent or vestigial (Zhang and Feng, 2004). The m1 of *P. brevirostris licenti* from Fanchang Renzidong has a vestigial metaconid, and its talonid has a prominent hypoconid and entoconid, but the hypoconulid is vestigial (Liu and Qiu, 2009). The *P. licenti* from XSG of Nihewan has a similar paraconid and protoconid to that of the SSMZ specimen, but with entoconid and hypoconulid except the hypoconid, i.e. with more talonid cuspids (Teilhard de Chardin and Piveteau, 1930). Pei (1987) examined 15 specimens of m1 of *Pachycrocuta licenti* from the Liucheng *Gigantopithecus* Cave, only 3 of which have metaconids, and 13 of which have both hypoconid and entoconid. Pei also proposed that the reduction of the metaconid-talonid complex on m1 is the general tendency in the evolution of *Pachycrocuta-Crocuta* during the Quaternary Period.

The SSMZ specimen is different from that of *Crocuta honanensis* of Early Pleistocene age in its larger size and developed cusplets on the lower premolars, and complicated dp3; while the P4 of the latter has a relatively large protocone and small parastyle, m1 with a small and low paraconid, but high and larger protoconid, and a well developed talonid with hypoconid and entoconid (Pei, 1934), the widest part of m1 occurs at the middle part rather than at the paraconid blade (Qiu et al., 2004). *Crocuta honanensis* was one element of the CNF, and it is also the oldest non-African *Crocuta* presently known (Lewis and Werdelin, 2022).

Compared with the recently reported Late Pliocene *P. pyrenaica* from the Yegou site (Liu et al., 2022), the latter has better-developed metaconid and talonid on m1.

Moreover, both the dp4 and m1 of the SSMZ materials are more primitive, according to Werdelin and Solounias (1991), than those of the *P. sinensis* from ZKD Loc.1, but similar to those of *P. licenti* of the Early Pleistocene faunas.

A partial mandible of a large carnivoran from SSMZ was originally identified as *Panthera* sp. (Tong et al., 2021). Currently, it is reidentified as *Pachycrocuta licenti* because of its large size and characters of the angular process. Furthermore, the coronoid process of the SSMZ specimen is different from that of the contemporary *Panthera palaeosinensis* (Zdansky, 1924: Pl. XXXII, Figs. 3 and 4) in its curved form of the summit. On the other hand, during the time span of Early Pleistocene, there was no such a big sized pantherine in China, the ramus height is only 85.4 for *Panthera zdanski* (Mazák et al., 2011) and 78.5 for *Panthera palaeosinensis* (Mazák, 2010), both of them represent the earliest record of tiger-like *Panthera* as known up to now. The ramus height of SSMZ specimen is close to those of *Pachycrocuta* spp. (Table 6).

It is worth mentioning that the Chinese giant hyenas, including *Pachycrocuta licenti* and *P. sinensis*, are included in the European species *Pachycrocuta brevirostris*, and the original specific names were retained as subspecies (Liu et al., 2021). This classification scheme, however, is yet to be widely accepted.

Concerning the lower deciduous dentitions, Teilhard de Chardin and Piveteau (1930) once proposed that the dp3 of *Crocuta honanensis* from Xiashagou resembles that of a felid rather than hyena. Actually, hyaenid dp4 is different from that of a tiger in its larger size and better-developed

Table 6
Measurements of the mandibular ramus of *Pachycrocuta licenti*, compared with related taxa.

	Ramus height at coronoid process	Ramus height at condyle	TD of condyle	Sources
Pachycrocuta licenti	112.8	45.3	55.3	V 31922, this paper
Pachycrocuta licenti	95–104			Qiu et al. (2004)
Pachycrocuta brevirostris	114[a]			Iannucci et al. (2022)
Pachycrocuta brevirostris licenti	84			Liu and Qiu (2009)
Pachycrocuta brevirostris	?123.6			Turner and Anton,1996
Pachycrocuta perrieri	91.8		43.7	Argant (2004)
Acinonyx pardinensis pleistocaenicus	90–91.5			Hemmer (2001)
Acinonyx pardinensis	74.0			Cherin et al. (2014b)
Panthera palaeosinensis	78.5			Mazák (2010)
Panthera zdanskyi	85.4			Mazák et al. (2011)
Panthera gombaszogensis	99.0			Argant and Argant (2011)
Panthera tigris	ca. 105		ca. 45	Tiwari et al. (2011)
Panthera leo	97.9 (wild), 87.8 (captive)			Zuccarelli (2004)

[a] Obtained by measuring Fig. 5 of Iannucci et al. (2022) by the first author of the present paper.

talonid. On the other hand, the dp4 of *Panthera tigris* has a developed metaconid and its talonid has the form of a pointed cuspid (Pei, 1934; Baryshnikov, 2016).

The partial mandible is referred to *Pachycrocuta licenti* because of its high ramus and the less pronounced inferior boundary of the masseteric fossa.

5. Discussions

The carnivore guild of the CNF is dominated by canids (Teilhard de Chardin and Piveteau, 1930), which is reconfirmed at the SSMZ site. In the Nihewan fauna, the canid fossils are rich and diverse, with 3 genera and 5 species having been reported up to now: *Canis chihliensis, Canis palmidens, Eucyon minor, Vulpes chikushanensis, Nyctereutes sinensis* (or *Nyctereutes schlosseri*). It is worth mentioning that the recent excavations at the Yangshuizhan site in Nihewan Basin (*sensu lato*) resulted in the discovery of a large quantity of fossil raccoon dogs (*Nyctereutes sinensis*), including 24 skulls and 39 mandibles (Liu, 2019). In the SSMZ fauna, *Canis chihliensis* is the most common carnivoran whose fossil specimens include crania, mandibles and most parts of the postcranial skeleton, which represent the most informative collection for Early Pleistocene *Canis* in China. The species *C. chihliensis* is a hypercarnivorous species (Tong et al., 2020), which is characterized by its reduced metaconid and entoconid in m1, which may indicate a close relationship with *Xenocyon dubius*. It seems that *C. chihliensis* stands at the crossroad between *Canis* and *Cuon*, but its relationship with the Middle Pleistocene *Canis mosbachensis variabilis* is still uncertain. The Chinese wolf of Middle Pleistocene epoch was compared with the contemporary European wolf *Canis mosbachensis* (Sotnikova, 2001; Tedford et al., 2009), and a recent study even treated the Chinese *C. variabilis* as a subspecies of the European species *Canis mosbachensis* (Jiangzuo et al., 2018), which means the Middle Pleistocene *Canis* fauna in North China probably had a European origin.

In the Nihewan fauna, bear fossils are very scanty, with only two specimens of *Ursus etruscus*, one partial maxilla and one isolated M2, having ever been reported (Teilhard de Chardin and Piveteau, 1930). Recently the small *Ursus* fossils of Early-Middle Pleistocene from North China were grouped under a new subspecies *Ursus etruscus orientalis* Jiangzuo et al. (2017). The bear fossil is absent in the SSMZ fauna. The rareness of *Ursus* fossils in the Nihewan fauna can be regarded as one of the important features to distinguish it from the later Zhoukoudian fauna. In China, the Early Pleistocene ursids are rare in fossil, but are complicated in taxonomy (Qiu et al., 2009).

Although several mustelids (*Eirictis*, *Meles*, *Lutra* and *Martes*) from Nihewan Basin had been reported (Teilhard de Chardin and Piveteau, 1930; Tang et al., 1995; Qiu, 2006), they were poorly represented in fossil records, and they are absent in SSMZ.

In the Nihewan fauna, two kinds of hyenas have been recognized: *Pachycrocuta licenti* and *Crocuta honanensis* (Qiu et al., 2004). The SSMZ hyena fossils can be referred to *Pachycrocuta licenti* because of their larger size and developed lower premolar cusplets as well as the form of m1.

The important felid fossils of the Nihewan fauna include *Homotherium crenatidens*, *Megantereon nihowanensis* and the early *Acinonyx* (including *Sivapanthera*), all of them being represented by nearly complete skulls and mandibles (Teilhard de Chardin and Piveteau, 1930; Qiu et al., 2004; Chen et al., 2017; Tong et al., 2021). True cats, both the pantherines and felines, are poorly recorded, except the *Lynx*. *Panthera* are absent in the Nihewan fauna, although the earliest fossil record of *Panthera* in China can be traced back to 2.55–2.16 Ma in the Longdan fauna (Qiu et al., 2004; Mazák et al., 2011).

Although all of the SSMZ carnivoran taxa are the common elements in the CNF, the recently unearthed postcranial skeletons of *Canis chihliensis* and *Acinonyx* represent the first knowledge for their kinds, and the fossil materials of *Canis chihliensis* from SSMZ represent the best collection for this species. In taxonomic composition, including both carnivores and ungulates, the SSMZ fauna shares the majority of its taxa with the XSG fauna (Tong et al., 2021), which means the SSMZ fauna very probably has the same geologic age with the XSG fauna, but maybe slightly younger according to the provisional character analysis for some taxa, e.g., *Canis* and *Pachycrocuta*.

The carnivore guild of the Nihewan fauna has high similarity with those of the Dmanisi fauna. If the transfer of *pachygnatha* from *Mustela* to *Pannonictis* (Sotnikova, 1980; García et al., 2008; Colombero et al., 2012) is correct, Dmanisi fauna shares 12 taxa of its 14 carnivoran taxa (*Homotherium latidens*, *Megantereon whitei*, *Panthera onca georgica*, *Acinonyx pardinensis*, *Lynx issiodorensis*; *Pachycrocuta brevirostris*; *Canis* (*Xenocyon*) *lycaonoides*, *Canis borjgali*, *Vulpes alopecoides*; *Ursus etruscus*; *Lutra* sp., *Martes* sp., *Meles* sp., and *Pannonictis* sp., Bartolini-Lucenti et al., 2022aa,b) with the Nihewan fauna at the generic level; although the determination of the species "*pachygnatha*" is still controversial, and others placed it under the recently established genus *Eirictis* (Qiu et al., 2004).

Among the SSMZ carnivore guild, *Canis chihliensis* and *Acinonyx* sp. are of the most significance in age determination. *Canis chihliensis* has reduced protocone on P4, prominent parastyle on M1, relatively larger M2, crest-like buccal cusps, and reduced lingual cuspids on m1, all of which are related to hypercarnivorous adaptations and are distinct from the Mid-Late Pleistocene *Canis* species (Tong et al., 2020). Although the giant cheetah *A. pardinensis* appeared in western Europe a little over 3 Ma (Werdelin and Peigné, 2010), their fossil records in Eurasia are mainly limited to the Early Pleistocene epoch (Cherin et al., 2014b). Cheetahs from the Nihewan Basin suggest that North China can be regarded as a center of evolution for these predators not only for the rich fossil records but also for their morphological variations. The SSMZ carnivoran guild shares quite a number of elements with the contemporary European faunas between 2.0 and 1.8 Ma (Konidaris, 2022), which shows that the mammalian fauna communicated frequently during the Early Pleistocene over the continental Eurasia.

In conclusion, the SSMZ fauna shares all of its carnivoran taxa with those of the CNF and the Dmanisi fauna at the generic level, which means they should share approximately the same geologic age, or the SSMZ fauna is slightly younger than the CNF according to the *Canis* and hyaenid fossils. Like the Dmanisi fauna (Belmaker, 2018), the *Canis*-dominated carnivoran guild of SSMZ fauna also indicates an open grassland/shrubland habitat.

6. Conclusions

In the SSMZ fauna, the carnivore guild includes *Canis chihliensis*, *Nyctereutes* sp., *Homotherium* sp., *Acinonyx* sp., *Lynx shansius* and *Pachycrocuta licenti*, among which *C. chihliensis* is the dominant and best represented species whose fossil materials include crania, mandibles and postcranial skeletons. Fossils of *C. chihliensis* from SSMZ thus represent the best collection for this species ever known, and the postcranial skeletons represent the only knowledge for the Early Pleistocene *Canis* in China. The second important taxon is the giant cheetah *Acinonyx* sp., whose postcranial skeletons represent the richest and only collection for its kind in the geologic age in China. The Nihewan Basin can be regarded as an important spot for the evolution of early cheetahs not only for its rich fossil records but also for its morphological variations. The carnivore guild of SSMZ fauna resembles the CNF and the Dmanisi fauna to a considerable degree, which means they should have approximately the same geologic age, or slightly younger than the CNF according to the *Canis* and hyaenid fossils. The SSMZ carnivoran guild shares quite a number of elements with the contemporary European faunas, which shows that the mammalian fauna once communicated frequently during the Early Pleistocene over the continental Eurasia. In faunal composition, the SSMZ fauna is closer to the XSG fauna; while in stratigraphic correlation, the SSMZ fauna is closer to XCL fauna.

Author contributions

Haowen Tong: Fossil excavation; conceptualization; data collection and analysis; manuscript drafting; final approval. **Bei Zhang**: Fossil excavation; CT scan data processing; made some minor corrections on the main text; final approval**. Xi Chen**: Fossil excavation; made some minor corrections on the main text; final approval. **Qigao Jiangzuo**: Made some corrections and modifications on the main text; final approval. Jinyi Liu: reconfirmation of some fossils' identification, contributed some ideas on the discussion of *Canis* evolution, final approval. **Xiaoming Wang**: Made extensive corrections on the whole text and improved the English text; final approval.

Data availability

Data are included within the submitted article and supplementary materials.

Declaration of competing interest

The authors declare that they have no known competing financial interests or personal relationships that could have appeared to influence the work reported in this paper.

Acknowledgements

The authors wish to express their thanks to the following people and organizations for their help: Wei Q., Han F., Sun B. Y., Chen X., Wang X. M., Lü D., Sun J. J., Xu Z. J., Qiu Z. W., Wang Q. Y., Sun B. H., Hu N., Liu X. T. and Yin C. for participating the excavations; Qiu Z. X. for fruitful discussions; Werdelin L. for sharing his publications; Hou Y. M. for CT scanning. This work was supported by the following grants: the National Natural Science Foundation of China (Grant Nos. 42172021, 41572003); the Strategic Priority Research Program of Chinese Academy of Sciences (Grant No. XDB26000000) and the National Key R & D Program of China (Grant No. 2020YFC1521500).

Appendix A. Supplementary data

Supplementary data to this article can be found online at https://doi.org/10.1016/j.quaint.2023.04.003.

References

Antón, M., Salesa, M.J., Galobart, A., Tseng, Z.J., 2014. The Plio-Pleistocene scimitar-toothed felid genus *Homotherium* Fabrini, 1890 (Machairodontinae, Homotherini): diversity, palaeogeography and taxonomic implications. Quat. Sci. Rev. 96, 259–268.

Antón, M., Galobart, A., Turner, A., 2005. Co-existence of scimitartoothed cats, lions and hominins in the European Pleistocene. Implications of the post-cranial anatomy of *Homotherium latidens* (Owen) for comparative palaeoecology. Quat. Sci. Rev. 24, 1287–1301.

Argant, A., 2004. Les carnivores du gisement Pliocène final de Saint-Vallier (Drôme, France). Geobios 37, S133–S182.

Argant, A., Argant, J., 2011. The *Panthera gombaszogensis* story: the contribution of the château brecciama (Saône-et-Loire, burgundy, France). Quaternaire, Hors-série 4, 247–269.

Azzaroli, A., 1983. Quaternary mammals and the "End-Villafranchian" dispersal event. A turning point in the history of Eurasia. Palaeogeogr. Palaeoclimatol. Palaeoecol. 44, 117–139.

Barnett, R., Barnes, I., Phillips, M.J., Martin, L.D., Harington, C.R., Leonard, J.A., Cooper, A., 2005. Evolution of extinct sabre-tooths and the American cheetah-like cat. Curr. Biol. 15, R589–R590.

Bartolini-Lucenti, S., Alba, D.M., Rook, L., Moyà-Solà, S., Madurell-Malapeira, J., 2017. Latest early Pleistocene wolf-like canids from the iberian Peninsula. Quat. Sci. Rev. 162, 12–25.

Bartolini-Lucenti, S., Cirilli, O., Pandolfi, L., Bernor, R.L., Bukhsianidze, M., Carotenuto, F., Lordkipanidze, D., Tsikaridze, N., Rook, L., 2022b. Zoogeographic significance of Dmanisi large mammal assemblage. J. Hum. Evol. 163, 103125 https://doi.org/10.1016/j.jhevol.2021.103125.

Bartolini-Lucenti, S., Madurell-Malapeira, J., Martínez-Navarro, B., Cirilli, O., Pandolfi, L., Rook, L., Bushkhianidze, M., Lordkipanidze, D., 2022a. A comparative study of the Early Pleistocene carnivore guild from Dmanisi (Georgia). J. Hum. Evol. 162, 103108 https://doi.org/10.1016/j.jhevol.2021.103108.

Bartolini-Lucenti, S., Madurell-Malapeira, J., Martínez-Navarro, B., Palmqvist, P., Lordkipanidze, D., Rook, L., 2021. The early hunting dog from Dmanisi with comments on the social behaviour in Canidae and hominins. Sci. Rep. 11, 13501 https://doi.org/10.1038/s41598-021-92818-4.

Bartolini-Lucenti, S., Rook, L., Morales, J., 2018. *Nyctereutes* (Mammalia, Carnivora, Canidae) from layna and the eurasian raccoon-dogs: an updated revision. Riv. Ital. Paleontol. Stratigr. 124 (3), 597–616.

Bartolini-Lucenti, S., Spassov, N., 2022. Cave canem! The earliest *Canis* (*Xenocyon*) (Canidae, Mammalia) of Europe: taxonomic affinities and paleoecology of the fossil wild dogs. Quat. Sci. Rev. 276, 107315 https://doi.org/10.1016/j.quascirev.2021.107315.

Baryshnikov, G.F., 2014. Late Pleistocene hyena *Crocuta ultima ussurica* (Mammalia: Carnivora: Hyaenidae) from the paleolithic site in geographical society cave in the Russian far East. Proc. Zool. Inst. RAS 318 (3), 197–225.

Baryshnikov, G.F., 2016. Late Pleistocene Felidae remains (Mammalia, Carnivora) from geographical society cave in the Russian far East. Proc. Zool. Inst. RAS 320 (1), 84–120.

Bellani, G.G., 2020. Felines of the World: Discoveries in Taxonomic Classification and History. Academic Press, London, pp. 1–476.

Belmaker, M., 2018. Insights from carnivore community composition on the paleoecology of Early Pleistocene Eurasian sites: implications for the dispersal of hominins out of Africa. Quat. Int. 464, 3–17.

Brugal, J.P., Boudadi-Maligne, M., 2011. Quaternary small to large canids in Europe: taxonomic status and biochronological contribution. Quat. Int. 243, 171–182.

Chen, X., Tong, H.W., 2017. On the hindfoot bones of *Mammuthus trogontherii* from Shanshenmiaozui in Nihewan Basin, China. Quat. Int. 445, 50–59.

Chen, X., Zhao, H.L., Zhang, B., Tong, H.W., 2017. Excavation and faunal report of the early Pleistocene Shigou site B in Nihewan Basin, north China. Quat. Sci. 37 (4), 895–907.

Cherin, M., Bertè, D.F., Rook, L., Sardella, R., 2014a. Re-defining *Canis etruscus* (Canidae, Mammalia): a new look into the evolutionary history of Early Pleistocene dogs resulting from the outstanding fossil record from Pantalla (Italy). J. Mamm. Evol. 21, 95–110.

Cherin, M., Iurino, D.A., Sardella, R., Rook, L., 2014b. *Acinonyx pardinensis* (Carnivora, Felidae) from the early Pleistocene of pantalla (Italy): predatory behavior and ecological role of the giant plio–pleistocene cheetah. Quat. Sci. Rev. 87, 82–97.

Cherin, M., Bertè, D.F., Sardella, R., Rook, L., 2013. *Canis etruscus* (Canidae, Mammalia) from Pantalla (Perugia, central Italy): an element of the late Villafranchian large carnivore guild of Italy. Boll. Soc. Paleontol. Ital. 52 (1), 11–18.

Cherin, M., Iurino, D.A., Zanatta, M., Fernandez, V., Paciaroni, A., Petrillo, C., Rettori, R., Sardella, R., 2018. Synchrotron radiation reveals the identity of the large felid from Monte Argentario (Early Pleistocene, Italy). Sci. Rep. 8, 8338. https://doi.org/10.1038/s41598-018-26698-6.

Christiansen, P., Adolfssen, J.S., 2007. Osteology and ecology of*Megantereon cultridens* SE311 (Mammalia; Felidae; Machairodontinae), a sabrecat from the late Pliocene - early Pleistocene of Senéze. France. Zool. J. Linn. Soc. 151 (4), 833–884.
Christiansen, P., Mazák, J., 2009. A primitive Late Pliocene cheetah and evolution of the cheetah lineage. Proc. Natl. Acad. Sci. USA 106, 512–515.
Colbert, E.H., Hooijer, D.A., 1953. Pleistocene mammals from the limestone fissures of Szechuan, China. Bull. Am. Mus. Nat. Hist. 102 (1), 1–134.
Colombero, S., Pavia, M., Rook, L., 2012. *Pannonictis nestii* (Galictinae, Mustelidae), a new element in the vertebrate association of the human site of Pirro Nord (Italy, Early Pleistocene). Geodiversitas 34 (3), 665–681.
Cueto, M., Camarós, E., Castaños, P., Ontañón, R., Arias, P., 2016. Under the skin of a lion: unique evidence of Upper Paleolithic exploitation and use of cave lion (*Panthera spelaea*) from the Lower Gallery of La Garma (Spain). PLoS One 11 (10), e0163591. https://doi.org/10.1371/journal.pone.0163591.
Day, L.M., Jayne, B.C., 2007. Interspecific scaling of the morphology and posture of the limbs during the locomotion of cats (Felidae). J. Exp. Biol. 210 (4), 642–654.
Diedrich, C.G., 2011. Late Pleistocene *Panthera leo spelaea* (Goldfuss, 1810) skeletons from the Czech Republic (central Europe); their pathological cranial features and injuries resulting from intraspecific fights, conflicts with hyenas, and attacks on cave bears. Bull. Geosci. 86 (4), 817–840.
Evans, H.E., Christensen, G.C., 1979. In: Miller's Anatomy of the Dog, second ed. W.B. Saunders Company, Philadelphia, pp. 1–1233.
Farjand, A., Zhang, Z.Q., Kaakinen, A., Bi, S.D., Gibbard, P.L., Wang, L.H., 2023. Rediscovery and stratigraphic calibration of the classic nihewan fauna, Hebei Province, China. Quat. Int. 646, 1–10.
García, N., Arsuaga, J.L., de Castro, J.M.B., Carbonell, E., Rosas, A., Huguet, R., 2008. The Epivillafranchian carnivore *Pannonictis* (Mammalia, Mustelidae) from Sima del Elefante (Sierra de Atapuerca, Spain) and a revision of the Eurasian occurrences from a taxonomic perspective. Quat. Int. 179, 42–52.
Geraads, D., 2014. How old is the cheetah skull shape? The case of *Acinonyx pardinensis* (Mammalia, Felidae). Geobios 47, 39–44.
Ghezzo, E., Rook, L., 2015. The remarkable *Panthera pardus* (Felidae, Mammalia) record from Equi (Massa, Italy): taphonomy, morphology, and paleoecology. Quat. Sci. Rev. 110, 131–151.
Gonyea, W.J., 1978. Functional implications of felid forelimb anatomy. Acta Anat. 102 (2), 111–121.
Gonyea, W.J., Ashworth, R., 1975. The form and function of retractile claws in the Felidae and other representative carnivorans. J. Morphol. 145, 229–238.
Hartstone-Rose, A., Werdelin, L., De Ruiter, D.J., Berger, L.R., Churchill, S.E., 2010. The Plio-Pleistocene ancestor of wild dogs, *Lycaon sekowei* n. sp. J. Paleontol. 84 (2), 299–308.
Hemmer, H., Kahlke, R.D., 2022. New results on felids from the early Pleistocene site of Untermassfeld. In: Kahlke, R.-D. (Ed.), The Pleistocene of Untermassfeld Near Meiningen (Thüringen, Germany), Part 5. Monogr, vol. 40. Römisch-Germanischen Zentralmuseums Mainz, pp. 1465–1566, 5.
Hemmer, H., 2001. Die Feliden aus dem Epivillafranchium von Untermaßfeld. In: Kahlke, R.-D. (Ed.), Das Pleistozän von Untermaßfeld bei Meiningen (Thüringen), Teil 3. Monogr, vol. 40. Römisch-Germanischen Zentralmuseums Mainz, pp. 699–782, 3.
Hemmer, H., Kahlke, R.D., Vekua, A.K., 2011. The cheetah *Acinonyx pardinensis* (Croizet et Jobert, 1828) s.l. at the hominin site of Dmanisi (Georgia) – a potential prime meat supplier in Early Pleistocene ecosystems. Quat. Sci. Rev. 30 (19–20), 2703–2714.
Homberger, D.G., Ham, K., Ogunbakin, T., Bonin, J.A., Hopkins, B.A., Osborn, M.L., Hossain, I., Barnett, H.A., Matthews II, K.L., Butler, L.G., Bragulla, H.H., 2009. The structure of the cornified claw sheath in the domestic cat (*Felis catus*): implications for the claw shedding mechanism. J. Anat. 214, 620–643.
Hopwood, A.T., 1947. Contributions to the study of some african mammals—III. Adaptations in the bones of the fore-limb of the lion, leopard, and cheetah. J. Linn. Soc. Lond. Zool. 41, 259–271.
Hu, C.K., Qi, T., 1978. Gongwangling Pleistocene mammalian fauna of lantian, Shaanxi. Palaeontol. Sin. Ser. C 21, 36–39 (in Chinese with English summary).
Iannucci, A., Mecozzi, B., Kahlke, R.-D., Sardella, R., 2022. New results on hyaenids from the early Pleistocene site of Untermassfeld. In: Kahlke, R.-D. (Ed.), The Pleistocene of Untermassfeld Near Meiningen (Thüringen, Germany), Part 5. Monogr, Römisch-Germanischen Zentralmuseums Mainz, vol. 40, pp. 1403–1422, 5.
Jiangzuo, Q.G., 2021. Geographical and chronological distribution of Chinese Pleistocene large canids: current status and prospects. Chin. Sci. Bull. 66, 1426. https://doi.org/10.1360/TB-2020-0690 (in Chinese with English abstract).
Jiangzuo, Q.G., Li, L., Madurell-Malapeira, J., Wang, S.Q., Li, S.J., Fu, J., Chen, S.Q., 2022a. The diversification of the *Lynx* lineage during the Plio-Pleistocene—evidence from a new small *Lynx* from Longdan, Gansu Province, China. Biol. J. Linn. Soc. 136 (4), 536–551. https://doi.org/10.1093/biolinnean/blac054.
Jiangzuo, Q.G., Liu, J., Wagner, J., Dong, W., Chen, J., 2018. Taxonomical revision of fossil *Canis* in Middle Pleistocene sites of Zhoukoudian. Beijing, China and a review of fossil records of *Canis mosbachensis variabilis* in China. Quat. Int. 482, 93–108.
Jiangzuo, Q.G., Liu, J.Y., Wang, Y., Jin, C.Z., Liu, S.Z., Liu, J.Y., Chen, J., 2017. New materials of *Ursus etruscus* from Jinyuan cave of Luotuo Hill, Dalian and a brief review of *Ursus* cf. *etruscus* in China. Quat. Sci. 37, 828–837 (in Chinese with English abstract).
Jiangzuo, Q.G., Wang, Y., Song, Y., Liu, S., Jin, C., Liu, J., 2022b. Middle Pleistocene *Xenocyon lycaonoides* Kretzoi, 1938 in northeastern China and the evolution of *xenocyon-lycaon* lineage. Hist. Biol. https://doi.org/10.1080/08912963.2021.2022138.
Jiangzuo, Q.G., Zhao, H.L., Chen, X., 2022c. The first complete cranium of *Homotherium* (Machairodontinae, Felidae) from the Nihewan Basin (northern China). Anat. Rec. 2022, 1–11. https://doi.org/10.1002/ar.25029.
Johnson, W.E., Eizirik, E., Pecon-Slattery, J., Murphy, W.J., Antunes, A., Teeling, E., O'Brien, S.J., 2006. The Late Miocene radiation of modern Felidae: a genetic assessment. Science 311 (5757), 73–77.
Kitchener, A.C., Breitenmoser-Wursten, Ch, Eizirik, E., Gentry, A., Werdelin, L., Wilting, A., Yamaguchi, N., Abramov, A.V., Christiansen, P., Driscoll, C., Duckworth, J.W., Johnson, W., Luo, S.J., Meijaard, E., O'Donoghue, P., Sanderson, J., Seymour, K., Bruford, M., Groves, C., Hoffmann, M., Nowell, K., Timmons, Z., Tobe, S., 2017. A revised taxonomy of the Felidae. The final report of the cat classification task force of the IUCN/SSC cat specialist group. Cat News Spec. Issue 11, 1–80.
Kitchener, A.C., van Valkenburgh, B., Yamaguchi, N., 2010. Felid form and function. In: Macdonald, D.W., Loveridge, A.J. (Eds.), Biology and Conservation of Wild Felids. Oxford University Press, Oxford, pp. 83–106.
Konidaris, G., 2022. Guilds of large carnivorans during the Pleistocene of Europe: a community structure analysis based on foraging strategies. Lethaia 55 (2), 1–18.
Koufos, G.D., 2014. The Villafranchian carnivoran guild of Greece: implications for the fauna, biochronology and paleoecology. Integr. Zool. 9 (4), 444–460.
Koufos, G.D., Kostopoulos, D.S., 2016. The plio-pleistocene large mammal record of Greece: implications for early human dispersals into Europe. In: Harvati, K., Roksanic, M. (Eds.), Palaeoanthropology of the Balkans and Anatolia: Human Evolution and its Context. Springer, Dordrecht, pp. 269–280.
Kurtén, B., 1956. The status and affinities of *Hyaena sinensis* Owen and *Hyaena ultima* Matsumoto. Am. Mus. Novit. 1764, 1–48.
Lewis, M., Werdelin, L., 2022. A revision of the genus *Crocuta* (Mammalia, Hyaenidae). Palaeontograph. Abteilung 322. https://doi.org/10.1127/pala/2022/0120.
Liu, J.Y., Zhang, Y.Q., Chi, Z.Q., Wang, Y., Yang, J.S., Zheng, S.H., 2022. A late Pliocene *Hipparion houfenense* fauna from Yegou, Nihewan Basin and its biostratigraphic significance. Vert. PalAsiat. 60 (4), 278–323.
Liu, J.Y., Fang, Y.S., Zhang, Z.H., 2007. Carnivora. In: nanjing museum and Institute of archaeology. In: Province, Jiangsu (Ed.), The Early Pleistocene Mammalian Fauna at Tuozi Cave, Nanjing, China. Science Press, Beijing, pp. 25–67.
Liu, J.Y., Liu, J.Y., Zhang, H.W., Wagner, J., Jiangzuo, Q.G., Song, Y.Y., Liu, S.Z., Wang, Y., Jin, C.Z., 2021. The giant short-faced hyena *Pachycrocuta brevirostris* (Mammalia, Carnivora, Hyaenidae) from Northeast Asia: a reinterpretation of subspecies differentiation and intercontinental dispersal. Quat. Int. 577, 29–51.
Liu, J.Y., Qiu, Z.X., 2009. Carnivora. In: Jin, C., Liu, J. (Eds.), Paleolithic Site—The Renzidong Cave, Fanchang, Anhui Province. Science Press, Beijing, pp. 220–282 (in Chinese with English summary).
Liu, P., Deng, C.L., Li, S.H., Cai, S.H., Cheng, H.J., Yuan, B.Y., Wei, Q., Zhu, R.X., 2012. Magnetostratigraphic dating of the Xiashagou fauna and implication for sequencing the mammalian faunas in the Nihewan Basin, north China. Palaeogeogr. Palaeoclimatol. Palaeoecol. 315, 75–85.
Liu, P., Wu, Z.J., Deng, C.L., Tong, H.W., Qin, H.F., Li, S.H., Yuan, B.Y., Zhu, R.X., 2016. Magnetostratigraphic dating of the Shanshenmiaozui mammalian fauna in the Nihewan Basin, north China. Quat. Int. 400, 202–211.
Liu, W.H., 2019. *Nyctereutes* from Hongya Yangshuizhan Locality at Nihewan Basin, and the Systematic Revision on the Genus *Nyctereutes*. Unpublished Ph. D. Thesis.. Institute of Vertebrate Paleontology and Paleoanthropology Chinese Academy of Science, Beijing, pp. 1–384 (in Chinese with English abstract).
Londei, T., 2000. The cheetah (*Acinonyx jubatus*) dewclaw: specialization overlooked. J. Zool. London 251, 535–547.
Martin, L.D., Gilbert, B.M., Adams, D.B., 1977. A cheetah-like cat in the North American Pleistocene. Science 195, 981–982.
MartÍn-Serra, A., Figueirido, B., Palmqvist, P., 2014. A Three-dimensional analysis of morphological evolution and locomotor performance of the carnivoran forelimb. PLoS One 9 (1), e85574. https://doi.org/10.1371/journal.pone.0085574.
Martínez-Navarro, B., Lucenti, S.B., Palmqvist, P., Ros-Montoya, S., Madurell-Malapeira, J., Espigares, M.P., 2021. A new species of dog from the early Pleistocene site of venta micena (orce, baza basin, Spain). Comptes Rendus Palevol 20 (17), 297–314. https://doi.org/10.5852/cr-palevol2021v20a17.
Martínez-Navarro, B., Rook, L., 2003. Gradual evolution in the African hunting dog lineage systematic implications. Comptes Rendus Palevol 2, 695–702.
Mattern, M.Y., McLennan, D.A., 2000. Phylogeny and speciation of felids. Cladistics 16 (2), 232–253.
Mazák, J.H., 2010. What is *Panthera palaeosinensis*? Mamm Rev. 40 (1), 90–102.
Mazák, J.H., Christiansen, P., Kitchener, A.C., 2011. Oldest known pantherine skull and evolution of the tiger. PLoS One 6 (10), e25483. https://doi.org/10.1371/journal.pone.0025483.
McKenna, M.C., Bell, S.K., 1997. Classification of Mammals above the Species Level. Columbia University Press, New York, pp. 1–631.
Meachen, J., Schmidt-Küntzel, A., Haefele, H., Steenkamp, G., Robinson, J.M., Randau, M., McGowan, N., Scantlebury, D.M., Marks, N., Maule, A., Marker, L., 2018. Cheetah specialization: physiology and morphology. In: Marker, L., Boast, L. K., Schmidt-Küntzel, A. (Eds.), Biodiversity of the World—Cheetahs: Biology and Conservation. Elsevier, San Diego, pp. 93–105.
Mecozzi, B., Iurino, D.A., Bertè, D.F., Sardella, R., 2017. *Canis mosbachensis* (Canidae, Mammalia) from the middle Pleistocene of contrada monticelli (putignano, apulia, southern Italy). Boll. Soc. Paleontol. Ital. 56 (1), 71–78.
Merriam, J.C., Stock, C., 1932. The Felidae of Rancho La Brea, vol. 422. Carnegie Inst. Washington Publ, pp. 1–231.
Morales, M.M., Giannini, N.P., 2013. Ecomorphology of the African felid ensemble: the role of the skull and postcranium in determining species segregation and assembling history. J. Evol. Biol. 26 (5), 980–992.

Pappa, S., Tsoukala, E., Lazaridis, G., Rabeder, G., 2005. Milk teeth of Quaternary carnivores from northern Greek caves: preliminary report. Neue Forschungen zum Hohlenbaren in Europa, Abh. Bd. 45, 169–182.
Pei, W.C., 1934. On the Carnivora from locality 1 of choukoutien. Palaeontol. Sin. Ser. C 8 (1), 1–216.
Pei, W.C., 1940. The Upper cave fauna of Choukoutien. Palaeont. Sin., New Ser. C (10), 1–84.
Pei, W.C., 1987. Carnivora, proboscidea and rodentia from Liucheng *Gigantopithecus* cave and other caves in Guangxi. Mem. Inst. Vertebr. Paleontol. Paleoanthropol. Acad. Sinica 18, 1–134 (in Chinese with English abstract).
Pocock, R.I., 1917. The classification of the existing Felidae. Ann. Mag. Nat. Hist. ser. 8 (20), 329–350.
Qiu, Z.X., 2006. Quaternary environmental changes and evolution of large mammals in North China. Vert. PalAsiat. 44 (2), 109–132.
Qiu, Z.X., Deng, T., Wang, B.Y., 2004. Early Pleistocene mammalian fauna from longdan, dongxiang, Gansu, China. Palaeont. Sin., New Ser. C 27, 1–198 (in Chinese with English summary).
Qiu, Z.X., Deng, T., Wang, B.Y., 2009. First bear material from Dongxiang, Gansu—addition to the Longdan mammalian fauna (2). Vert. PalAsiat. 47 (4), 245–264.
Qiu, Z.X., Qiu, Z.D., Deng, T., Li, C.K., Zhang, Z.Q., Wang, B.Y., Wang, X.M., 2013. Neogene land mammal stages/ages of China: toward the goal to establish an Asian land mammal stage/age scheme. In: Wang, X.M., Flynn, L.J., Fortelius, M. (Eds.), Fossil Mammals of Asia: Neogene Biostratigraphy and Chronology. Columbia University Press, New York, pp. 29–90.
Rawn-Schatzinger, V.M., Collins, R.L., 1981. Scimitar cats, *Homotherium serum* cope from gassaway fissure, cannon county, Tennessee and the North American distribution of *Homotherium*. J. Tenn. Acad. Sci. 56 (1), 15–19.
Rawn-Schatzinger, V., 1983. Development and eruption sequence of deciduous and permanent teeth in the saber-tooth cat*Homotherium serum*Cope. J. Vertebr. Paleontol. 3, 49–57.
Rook, L., 1994. The plio-pleistocene old world *Canis* (*Xenocyon*) ex gr. *falconeri*. Boll. Soc. Paleontol. Ital. 33, 71–82.
Roşu, P.M., Predoi, G., Belu, C., Georgescu, B., Dumitrescu, I., Raita, S.M., 2016. Morphometric biodiversity in cheetah thoracic limb bones: a case study. Scientific Works, Ser. C. Vet. Med. 62 (1), 41–45.
Rothwell, T., 2001. A partial skeleton of *pseudaelurus* (Carnivora: Felidae) from the nambé member of the tesuque formation, española basin, New Mexico. Am. Mus. Novit. 3342, 1–31.
Russell, A.P., Bryant, H.N., 2001. Claw retraction and protraction in the Carnivora: the cheetah (*Acinonyx jubatus*) as an atypical felid. J. Zool. 254, 67–76.
Salesa, M.J., Antón, M., Turner, A., Morales, J., 2010. Functional anatomy of the forelimb in *Promegantereon ogygia* (Felidae, Machairodontinae, Smilodontini) from the Late Miocene of Spain and the origins of the sabre-toothed felid model. J. Anat. 216, 381–396.
Sardella, R., Iurino, D.A., 2012. The latest early Pleistocene sabertoothed cat *Homotherium* (Felidae, Mammalia) from Monte peglia (umbria, central Italy). Boll. Soc. Paleontol. Ital. 51, 15–22.
Sardella, R., Palombo, M.R., 2007. The Pliocene-Pleistocene boundary: which significance for the so-called Wolf event? Evidences from Western Europe. Quaternaire 18, 65–71.
Senter, P., Moch, J.G., 2015. A critical survey of vestigial structures in the postcranial skeletons of extant mammals. PeerJ 3, e1439. https://doi.org/10.7717/peerj.1439.
Smith, H.F., Adrian, B., Koshy, R., Alwiel, R., Grossman, A., 2020. Adaptations to cursoriality and digit reduction in the forelimb of the African wild dog (*Lycaon pictus*). PeerJ 8, e9866. https://doi.org/10.7717/peerj.9866.
Sohel, M.S.H., Islam, K.N., Rahman, M.L., 2021. Anatomical features of some bones of the forelimbs of lions (*Panthera le*). Int. J. Morphol. 39 (2), 378–385.
Sotnikova, M., 1980. The late Pliocene mustelidae from shamar. Bull. Comm. Stud. Quat. 50, 138–145 (in Russian).
Sotnikova, M., 2001. Remains of Canidae from the lower Pleistocene site of Untermassfeld. In: Kahlke, R.D. (Ed.), Das Pleistozän von Untermassfeld bei Meiningen (Thüringen). Teil, Römisch-Germanisches Zentralmuseum, pp. 607–632.
Sotnikova, M.V., Dodonov, A.E., Pen'kov, A.V., 1997. Upper Cenozoic bio-magnetic stratigraphy of Central Asian mammalian localities. Palaeogeogr. Palaeoclimatol. Palaeoecol. 133, 243–258.
Spassov, N., 2011. *Acinonyx pardinensis* (Croizet et Jobert) remains from the Middle Villafranchian locality of Varshets (Bulgaria) and the Plio-Pleistocene history of the cheetahs in Eurasia. Estud. Geol. 67 (2), 245–253.
Sreeranjini, A.R., Ashok, N., 2008. Gross anatomical studies of the scapula in leopard (*Panthera pardus*). J. Vet. Anim. Sci. 39 (1), 47–48.
Sreeranjini, A.R., Ashok, N., Rajani, C.V., Indu, V.R., Maya, S., Lucy, K.M., Chungath, J. J., 2014. Gross anatomical studies on the radius and ulna of leopard (*Panthera pardus*). Indian Vet. J. 91 (11), 24–26.
Tang, Y.J., 1980. Note on a small collection of Early Pleistocene mammalian fossils from northern Hebei. Vert. PalAsiat. 18 (4), 314–323 (in Chinese with English summary).
Tang, Y.J., Li, Y., Chen, W.Y., 1995. Mammalian fossils and the age of Xiaochangliang paleolithic site of yangyuan. Hebei.Vert. PalAsiat. 33 (1), 74–83 (in Chinese with English summary).
Tedford, R.H., Qiu, Z.X., 1991. Pliocene *Nyctereutes* (Carnivora, Canidae) from Yushe, Shanxi, with comments on Chinese fossil raccoon-dogs. Vert. PalAsiat. 29, 176–189.
Tedford, R.H., Wang, X.M., Taylor, B.E., 2009. Phylogenetic systematics of the North American fossil Caninae (Carnivora: Canidae). Bull. Am. Mus. Nat. Hist. 325, 1–218.
Teilhard de Chardin, P., Leroy, P., 1945. Les felides de Chine. Publ. Inst. Geo-Biol. 11, 1–58.
Teilhard de Chardin, P., Pei, W.C., 1941. The fossil mammals from locality 13 of choukoutien. Palaeont. Sin., New Ser. C. No. 11, 1–118.
Teilhard de Chardin, P., Piveteau, J., 1930. Les mammiféres fossils de Nihowan (Chine). Ann. Paleontol. 19, 1–134.
Tiwari, Y., Taluja, J.S., Vaish, R., 2011. Biometry of mandible in tiger (*Panthera tigris*). Annu. Rev. Res. Biol. 1 (1), 14–21.
Tong, H.W., 2012. New remains of *Mammuthus trogontherii* from the early Pleistocene nihewan beds at Shanshenmiaozui, Hebei. Quat. Int. 255, 217–230.
Tong, H.W., Chen, X., 2016. On newborn calf skulls of early Pleistocene *Mammuthus trogontherii* from Shanshenmiaozui in Nihewan Basin, China. Quat. Int. 406, 57–69.
Tong, H.W., Chen, X., Zhang, B., 2017. New fossils of *Bison palaeosinensis* (artiodactyla, Mammalia) from the steppe mammoth site of early Pleistocene in Nihewan Basin, China. Quat. Int. 445, 250–268.
Tong, H.W., Chen, X., Zhang, B., 2018. New postcranial bones of *Elasmotherium peii* from Shanshenmiaozui in Nihewan Basin, northern China. Quaternaire 29 (3), 195–204.
Tong, H.W., Chen, X., Zhang, B., Rothschild, B., White, S., Balisi, M., Wang, X., 2020. Hypercarnivorous teeth and healed injuries to *Canis chihliensis* from Early Pleistocene Nihewan beds, China, support social hunting for ancestral wolves. PeerJ 8, e9858. https://doi.org/10.7717/peerj.9858.
Tong, H.W., Hu, N., Han, F., 2011a. A preliminary report on the excavations at the early Pleistocene fossil site of Shanshenmiaozui in Nihewan Basin, Hebei, China. Quat. Sci. 31, 643–653 (in Chinese with English summary).
Tong, H.W., Hu, N., Liu, J.Y., Clarke, R., 2011b. Inter-Regional comparisons on the Quaternary large mammalian faunas between China and sub-Saharan Africa. Acta Geol. Sin. 85 (1), 91–106.
Tong, H.W., Hu, N., Wang, X.M., 2012. New remains of *Canis chihliensis* (Mammalia, Carnivora) from Shanshenmiaozui, a lower Pleistocene site in yangyuan. Hebei. Vert. PalAsiat. 50 (4), 335–360.
Tong, H.W., Wang, F.G., Zheng, M., Chen, X., 2014. New fossils of *Stephanorhinus kirchbergensis* and Elasmotherium peii from the Nihewan Basin. Acta Anthropol. Sin. 33 (3), 369–388 (in Chinese with English summary).
Tong, H.W., Wang, X.M., 2014. Juvenile skulls and other postcranial bones of *Coelodonta nihowanensis* from Shanshenmiaozui, Nihewan Basin, China. J. Vertebr. Paleontol. 34 (3), 710–724.
Tong, H.W., Zhang, B., 2019. New fossils of *Eucladoceros boulei* (artiodactyla, Mammalia) from early Pleistocene nihewan beds, China. Palaeoworld 28 (3), 403–424.
Tong, H.W., Zhang, B., Chen, X., Wang, X.M., Sun, J.J., 2021. Chronological significance of the mammalian fauna from the early Pleistocene Shanshenmiaozui site in Nihewan Basin, northern China. Acta Anthropol. Sin. 40 (3), 469–489 (in Chinese with English abstract).
Tong, H.W., Zhang, B., Wu, X.Z., Qu, M.S., 2019. Mammalian fossils from the middle Pleistocene human site of bailongdong in yunxi, Hubei. Acta Anthropol. Sin. 38 (4), 613–640 (in Chinese with English abstract).
Tong, Y.S., Zheng, S.H., Qiu, Z.D., 1995. Cenozoic mammal ages of China. Vert. PalAsiat. 33 (4), 290–314 (in Chinese with English summary).
Turner, A., Anton, M., 1996. The giant hyaena *Pachycrocuta brevirostris* (Mammalia, Carnivora, Hyaenidae). Geobios 29 (4), 455–468.
Van Valkenburgh, B., Pang, B., Cherin, M., Rook, L., 2018. The cheetah: evolutionary history and paleoecology. In: Marker, L., Boast, L.K., Schmidt-Küntzel, A. (Eds.), Biodiversity of the World—Cheetahs: Biology and Conservation. Elsevier, San Diego, pp. 25–32.
Van Valkenburgh, B., Grady, F., Kurtén, B., 1990. The plio-pleistocene cheetah-like cat *Miracinonyx inexpectatus* of North America. J. Vertebr. Paleontol. 10 (4), 434–454.
Van Valkenburgh, B., Wang, X., Damuth, J., 2004. Cope's rule, hypercarnivory, and extinction in North American canids. Science 306 (5693), 101–104.
von den Driesch, A., 1976. A Guide to the Measurements of Animal Bone from Archaeological Sites. Peabody Museum Bulletin 1. Peabody Museum of Archaeology and Ethnology. Harvard University, Cambridge, pp. 1–137.
Wang, X., Li, Q., Xie, G., 2014. Earliest record of *Sinicuon* in Zanda Basin, southern Tibet and implications for hypercarnivores in cold environments. Quat. Int. 355, 3–10.
Wang, X.M., Tedford, R.H., Van Valkenburgh, B., Wayne, R.K., 2004. Ancestry: evolutionary history, molecular systematics, and evolutionary ecology of Canidae. In: Macdonald, D.W., Sillero-Zubiri, C. (Eds.), The Biology and Conservation of Wild Canids. Oxford University Press, New York, pp. 39–54.
Werdelin, L., 1981. The evolution of lynxes. Ann. Zool. Fenn. 18 (1), 37–71.
Werdelin, L., Peigné, S., 2010. Chapter 32: Carnivora. In: Werdelin, L., Sanders, W. (Eds.), Cenozoic Mammals of Africa. University of California Press, Berkeley, pp. 603–657.
Werdelin, L., Solounias, N., 1991. The Hyaenidae: taxonomy, systematics and evolution. Foss. Strata 30, 1–104.
Werdelin, L., Dehghani, R., 2011. Chapter 8: Carnivora. In: Harrison, T. (Ed.), Palaeontology and Geology of Laetoli: Human Evolution in Context, vol. 2. Springer, Dordrecht, pp. 189–232.
Werdelin, L., Yamaguchi, N., Johnson, W.E., O'Brien, S.J., 2010. Chapter 2: phylogeny and evolution of cats (Felidae). In: Macdonald, D.W., Loveridge, A.J. (Eds.), Biology and Conservation of Wild Felids. Oxford University, Oxford, UK, pp. 59–82.
Yalden, D.W., 1970. The functional morphology of the carpal bones in carnivores. Acta Anat. 77 (4), 481–500.
Zdansky, O., 1924. Jungtertiäre carnivoren chinas. Palaeontol. Sin. Ser. C 2 (1), 1–149.
Zdansky, O., 1925. Quartare Carnivoren aus Nord-China. Palaeontol. Sin. Ser. C 2 (2), 1–26.
Zhang, Z.Q., Feng, X.B., 2004. Carnivora bodwich, 1821. In: Zheng, S.H. (Ed.), Jianshi Hominid Site. Science Press, Beijing, pp. 233–250 (in Chinese with English summary).

Zheng, S.H., Han, D.F., 1993. Mammalian fossils. In: Zhang, S.S. (Ed.), Comprehensive Study on the Jinniushan Paleolithic Site, vol. 19. Mem. Inst. Vert. Paleontol. Paleoanthrop. Acad. Sin. N., pp. 43–127 (in Chinese with English summary).

Zhu, R.X., Hoffman, K.A., Potts, R., Deng, C.L., Pan, Y.X., Guo, B., Shi, C.D., Guo, Z.T., Yuan, B.Y., Hou, Y.M., Huang, W.W., 2001. Earliest presence of humans in northeast Asia. Nature 413, 413–417.

Zuccarelli, M.D., 2004. Comparative morphometric analysis of captive vs. wild African lion (*Panthera leo*) skulls. Bios 75, 131–138.